NASA Technical Paper 2584

May 1986

1249

Dynamic Measurement of Total Temperature, Pressure, and Velocity in the Langley 0.3-Meter Transonic Cryogenic Tunnel

Charles B. Johnson and
P. Calvin Stainback

NASA

NASA Technical Paper 2584

1986

Dynamic Measurement of Total Temperature, Pressure, and Velocity in the Langley 0.3-Meter Transonic Cryogenic Tunnel

Charles B. Johnson and
P. Calvin Stainback

Langley Research Center
Hampton, Virginia

National Aeronautics
and Space Administration

Scientific and Technical Information Branch

SUMMARY

There is theoretical and experimental evidence which indicates that a sudden or step change in the rate at which the liquid nitrogen is injected into the circuit of a cryogenic wind tunnel can cause a temperature front in the flow for several tunnel circuit times. A temperature front, which occurs at intervals equal to the circuit time, is a sudden increase or decrease in the temperature of the flow followed by a nearly constant temperature. Since these fronts can have an effect on the control of the tunnel as well as the time required to establish steady flow conditions in the test section of a cryogenic wind tunnel, tests were conducted in the settling chamber in the Langley 0.3-Meter Transonic Cryogenic Tunnel (0.3-m TCT) in which high response instrumentation was used to measure the possible existence of these temperature fronts. Three different techniques were used to suddenly change the rate of liquid nitrogen being injected into the tunnel and the results from these three types of tests showed that temperature fronts do not appear to be present in the 0.3-m TCT. Also included are the velocity and pressure fluctuations measured in the settling chamber downstream of the screens and the associated power spectra.

INTRODUCTION

The requirements to simulate full-scale flight Reynolds numbers in wind tunnels have prompted an effort to develop transonic wind tunnels with very high unit Reynolds numbers. This effort has led to the construction of the National Transonic Facility (NTF) at the Langley Research Center. This tunnel obtains high unit Reynolds numbers, in part, by decreasing the total temperature of the working fluid to cryogenic temperatures by injecting liquid nitrogen (LN_2) into the circuit. There is theoretical evidence by Tripp (ref. 1) and experimental evidence by Blanchard and Dor (ref. 2) which suggest that a step increase or decrease in the LN_2 injection rate into the circuit of cryogenic wind tunnels can cause temperature fronts in the flow for several tunnel circuit times. Flow simulation calculations by Tripp in reference 1, based on a mathematical model of the flow in the 0.3-m TCT, clearly show temperature fronts as a result of a 3-sec pulsed increase in the LN_2 injection rate from 0.75 kg/sec to 1.1 kg/sec. (See fig. 1.) The temperature fronts, which occur at intervals equal to the circuit time, are the nearly vertical decreases (and then increases) in temperature followed by a nearly constant temperature between the vertical front. Results from the ONERA/CERT (Office National d'etudes et de Recherches Aérospatiates/Center d'etudes et de Recherches de Toulouse) T'2 (ref. 2) injector-driven cryogenic wind tunnel (see fig. 2) show temperature fronts for a large step change in the LN_2 injection rate (i.e., LN_2 valve cut off from a relatively high LN_2 flow rate). The occurrence of temperature fronts in the T'2 tunnel, after a sudden closure of the LN_2 injection at a stagnation temperature of about 135 K, is not surprising since the tunnel is internally insulated with cork and the flow is driven by ejectors operated by air at 273 K. It seemed doubtful that temperature fronts, similar to those found in the T'2 tunnel, would exist in a fan-driven tunnel such as the Langley 0.3-Meter Transonic Cryogenic Tunnel (0.3-m TCT) made out of aluminum and insulated externally. However, because of the following reasons, an experimental investigation was undertaken to determine if these temperature fronts exist in the 0.3-m TCT: (1) the theoretical results of Tripp (ref. 1) and the experimental measurements of Blanchard and Dor both showed temperature fronts (see figs. 1 and 2), (2) temperature fronts could possibly impact the control of a

cryogenic wind tunnel in terms of increased LN_2 consumption and increased time to reach a steady-state condition, and (3) temperature fronts could possibly perturb the steady-state operation with spikes or discontinuities in the total temperature, resulting from even small changes in the LN_2 injection rate.

It is the purpose of this paper to present the results of temperature measurements, with rapid response instrumentation (i.e., a hot-wire probe), during a sudden change in the rate of LN_2 injection. The LN_2 injection was altered by three different control techniques which rapidly increased (or decreased) the amount of LN_2 injected into the tunnel. In addition to these temperature measurements, which were made during periods of rapidly changing total temperature, the results of velocity and pressure fluctuation measurements made in the settling chamber during conditions of steady-state flow are presented. The results of a limited study to determine if LN_2 droplets were present in the flow is also presented.

SYMBOLS

D	diameter of settling chamber
F	reduced frequency, $2\pi Df/\bar{u}$
f	frequency
GN_2	gaseous nitrogen
LN_2	liquid nitrogen
M	Mach number
N	number of blades on fan, 12
n	fan rotational speed
$P\left(\frac{\tilde{p}}{\bar{p}}\right)$, $P\left(\frac{\tilde{u}}{\bar{u}}\right)$	probability distributions of the normalized fluctuating pressures and velocities, respectively
p	pressure
R	Reynolds number per foot
T	temperature
t_c	circuit time
u	velocity parallel to centerline of settling chamber
$\frac{\tilde{u}}{\bar{u}}(F)$	$\frac{\tilde{u}}{\bar{u}}$ as a function of F
vc	valve command
γ	ratio of specific heats

Subscripts:

i	initial condition before change in LN_2 injection rate
sc	settling chamber
t	total conditions
∞	free-stream conditions in test section

Superscripts:

~	root-mean-square value
-	mean value

APPARATUS AND DATA REDUCTION

Facility, Test Conditions, and Tunnel Controls

The measurements were made in the settling chamber of the 0.3-m TCT. (See refs. 3 and 4.) A sketch of the tunnel is shown in figure 3(a). This facility is a fan-driven, closed-circuit wind tunnel using nitrogen as the working fluid. The injection of liquid nitrogen into the tunnel circuit, just downstream of the test section, allows cryogenic total temperatures to be obtained. For steady operating conditions, the heat of compression of the fan is removed by the injection of liquid nitrogen. (See fig. 3(a).) Under equilibrium conditions, the excess mass is removed from the circuit through an exhaust system located just upstream of the settling chamber. (See fig. 3(a).) The test section is 8 inches wide and 24 inches high with slots in the floor and ceiling. The tunnel can be operated over the following conditions:

$$1.1 \text{ atm} \leq p_t \leq 6.0 \text{ atm}$$

$$0.1 \leq M_\infty \leq 0.9$$

$$78 \text{ K} \leq T_t \leq 320 \text{ K}$$

The test conditions used for the present test were:

$$2.0 \text{ atm} \leq p_t \leq 5.8 \text{ atm}$$

$$0.3 \leq M_\infty \leq 0.8$$

$$140 \text{ K} \leq T_t \leq 280 \text{ K}$$

A schematic of the control system that regulates the total temperature, total pressure, and Mach number is shown in figure 3(b). The purpose of the control system is to rapidly and accurately set and hold constant with time the tunnel total

temperature and pressure and the test-section Mach number. The total temperature is regulated by the amount of liquid nitrogen injected into the tunnel through digital valves. These valves are microprocessor controlled and have a temperature feedback from a thermocouple located in the settling chamber (temperature loop (T-loop)). The LN_2 is injected downstream of the test section, just ahead of the first turn, through four nozzles spaced 90° apart around the circumference of the tunnel. The flow rate through each of the nozzles is controlled by a digital valve. The digital valves, which have a very fast response, are also used to accurately measure the flow rate of LN_2 into the tunnel. Each digital valve has a resolution of 1 in 1024 (i.e., 10 bit) and consists of a number of calibrated, binary-weighted elements operating either fully open or fully closed. The individual elements in the digital valves are solenoid actuated, with the command for the required flow area updated every 0.10 sec by the microprocessor. The digital valves have a full area control speed of 0.50 sec. (See refs. 5 and 6.)

The total pressure in the tunnel is adjusted by two hydraulically driven valves which are controlled by an analog signal from a microprocessor which has feedback from a pressure transducer connected to the settling chamber (pressure loop (P-loop)). The two valves are located in pipes which exhaust to the atmosphere from the low-speed end of the tunnel. (See fig. 3(a).) One of the pressure control valves has a calibrated step input control for coarse control and the other valve is a calibrated, proportionally variable valve for a fine control of pressure.

The test-section Mach number is controlled by a third microprocessor which controls the rotational speed of the fan and has a feedback control loop from a total-pressure gauge (connected to a probe upstream of the test section) and a static-pressure gauge (connected to a pressure orifice on the sidewall of the test section), from which the Mach number is calculated (Mach loop (M-loop)). Therefore, the control systems for total temperature, total pressure, and test-section Mach number each has a dedicated microprocessor and can be operated in either a manual mode or an automatic mode. In the automatic mode, the three individual microprocessors control the respective valves and motor speed based on the command set points for total temperature, total pressure, and Mach number. In the manual mode, the control valves are set to a given percent opening and the fan motor is set to a given rotational speed in rpm. For all the results presented in this paper for the time variation of total temperature, the pressure and Mach number microprocessors were operated in an automatic mode with constant command set point. Therefore, when the total temperature was changed, the changes in Mach number and total pressure were small.

Although no measurement records were taken of the simultaneous total pressure and Mach number variation during the time the total temperature was rapidly changing, the studies by Thibodeaux and Balakrishna in reference 7 predict that total-pressure fluctuations would remain less than 5 percent for comparable temperature excursions. In addition, visual observations during the present tests indicated that the changes in Mach number were small during the temperature excursions.

The simulation of Mach number in reference 7 in response to the changes in total temperature did not include the closed-loop feedback control that was incorporated in the tunnel Mach-loop controller for the tests described in this paper. Therefore, no quantitative assessment can be made of the Mach number response during the change in total temperature. However, visual observations during the tests indicated the change in Mach number was small during the changes in total temperature.

Hot-Wire Anemometer and Probe

A commercially available, constant temperature anemometer (DISA 55M system with 55M10CTA standard bridge) and hot-wire probe were used during the present test. The probe holder and probe were mounted in the settling chamber normal to the flow, with the probe on the centerline of the settling chamber. The needles, which supported the hot wire, were bent 90° so that the ends of the needles pointed upstream 0.75 in. from the axis of the probe holder. The hot wire, 0.00015 in. in diameter, was made from platinum-coated tungsten and was located about 7.75 in. downstream of the screens. (See ref. 3.) An overheat of 1.8 was used to measure the velocity fluctuations in the settling chamber where the overheat is defined as the ratio of hot resistance to the cold resistance of the hot wire. The overheat was varied by changing the bridge resistance. In order to dynamically measure the total temperature during the temperature front investigation, the overheat was reduced to 1.15.

Pressure Transducer

A commercially available pressure transducer (Endevco model number 8510-5) designed to operate at cryogenic temperatures was used to measure the fluctuating pressures at the wall of the settling chamber. The transducer was 0.125 in. in diameter with a slotted cover to protect the diaphragm. The transducer was a differential pressure gauge having a range of ±5 psi. A reference tube connected to the back side of the diaphragm sensed the mean static pressure in the settling chamber with about 10 ft of 0.040-in-diameter tubing to minimize pressure fluctuations on the back side of the diaphragm. The transducer was mounted flush to the inside surface of the settling chamber with a plug which was faired into the inside surface of the 4-ft-diameter settling chamber. The pressure transducer was calibrated for variations in both pressure and temperature.

Total-Temperature Variations

In order to investigate the existence of temperature fronts in the 0.3-m TCT caused by the variation of the injection rate of LN_2, the injection of LN_2 was varied in three ways. The first method, referred to as the "auto-ramp" mode, was achieved with the microprocessor operating in an automatic mode to control the total temperature. In this mode, the valve commands varied based on the command set point of total temperature. The auto-ramp method was performed by first establishing a steady-flow condition in the test section at a fixed total temperature, and then setting into the microprocessor controller a new total temperature 9 K lower than the steady-state value. The sudden decrease in total temperature occurred when the microprocessor executed the command and increased the LN_2 flow rate through the digital valves. During the time the tunnel was attaining the new lower temperature under the control of the microprocessor, the original steady-state temperature value was reset into the controller and the 9-K increase was initiated as a valve command when a total-temperature decrease of 9 K was reached. The change in temperature during this mode of operation was limited to 9 K because of LN_2 injection limits built into the controller. Data were taken until the original temperature was approached or reached.

The second method for changing the total temperature was referred to as the "manual step" mode which required the microprocessor controller to be set in a manual

mode (i.e., constant LN_2 valve command). After steady flow was established (at a constant valve command) in the test section, a new higher value for the valve command was dialed into the controller which called for an increased LN_2 flow rate into the tunnel. This change in the LN_2 injection rate ranged from 20 to 100 percent greater than the steady-state mass-flow injection rate. The decrease in total temperature was initiated by the microprocessor controller when it was manually activated and a maximum temperature change of 20 K was arbitrarily chosen. While the temperature was decreasing, the original valve command was set into the controller, and when the temperature was reduced by 20 K, the microprocessor controller was again activated in order to return to the original total temperature. Again data were recorded over the total time the temperature was changing.

The third method of rapidly changing total temperature consisted of shutting off the LN_2 injection valves and waiting for the total temperature to increase about 20 K. After this 20-K change in the total temperature, the original valve command was activated and the original temperature was approached in the manual mode at a given valve command.

During the time that the temperature controller was altering the flow of LN_2 into the tunnel, the microprocessor controllers for total pressure and Mach number were in the automatic mode and maintained a nearly constant total pressure and Mach number, as discussed earlier.

RESULTS AND DISCUSSION

Total-Temperature Measurements

For the temperature measurements in the settling chamber, the overheat of the hot-wire probe was maintained at 1.15. Based on the work of Kovásznay (ref. 8), it was assumed that at this value of the overheat, the wire responded predominantly to variations in total temperature. The mean voltages measured across the hot wire were calibrated with total temperatures measured with a platinum resistance thermometer, and the results of this calibration were used to convert the measured voltages to total temperatures. Thus the variation in hot-wire voltage was used to determine the total temperature in the settling chamber during the previously described three methods used for sudden changes in LN_2 injection rates (i.e., (1) auto ramp, (2) manual step, and (3) close LN_2 valves). The time rate of change of the mean voltages measured across the hot wire were recorded on a tape recorder, the taped data were digitized at a rate of 100 times/sec, and the temperatures were calculated from these digitized values.

Examples of the variation of total temperature with time for the three types of step changes are presented in figures 4 through 8 for a test-section Mach number of 0.70 with the microprocessors controlling total pressure and Mach number in the automatic mode. The data are presented for three different time scales with the first plot representing the variation of total temperature with time for a major portion of the time that the temperature was changing. However, for figures 4(a), 5(a), 6(a), 7(a), and 8(a), the time scale is too compressed to identify conclusively the existence or nonexistence of any temperature fronts; therefore, the time scale was expanded for 15 sec for all five figures, and only a portion of the temperature step is included in the second portion (i.e., (b) part) of the five figures. In an effort to get a direct comparison with the temperature front data from the ONERA/CERT T'2 wind tunnel shown in figure 2, the time scale was further expanded for 3 sec, starting just before the initial change in T_t occurred. The circuit time t_c

calculated from an equation developed by Balakrishna (ref. 6) is indicated in all the figures with the 15- and 3-sec expanded time scales. The equation for circuit time is a function of stagnation pressure, stagnation temperature, and test-section Mach number and is determined by dividing the expression for the total mass of gas in the tunnel by the mass rate of flow through the tunnel circuit.

The previously described auto-ramp method of suddenly changing the total temperature with a sudden change of LN_2 injection is shown in figure 4 with the entire sequence of events shown in figure 4(a) for a period of about 20 sec. The initial total temperature at time prior to point A in figure 4(a) was set at 141 K by the T-loop microprocessor in the automatic mode. At point A, a 132-K command was input into the microprocessor controller which immediately opened the four LN_2 valves to a nearly 100-percent open position which resulted in a rapid decrease in temperature. The original temperature set point of 141 K was set into the microprocessor as the total temperature approached point B. When the controller was again activated at point B (i.e., to return to a temperature of 132 K by reducing the valve opening), there was a rapid increase in temperature with an overshoot in temperature to point C. After point C, the microprocessor began to reduce the tunnel total temperature to the desired 141-K condition as noted by the temperature level at point D. The 15-sec expanded region noted in figure 4(a) is shown in figure 4(b) along with a tunnel circuit time of 0.89 sec. Based on a knowledge of the circuit time, no discernible temperature front could be detected in the 15-sec expanded region. Similarly the 3-sec expanded region shown in figure 4(c) indicated no temperature front after the sudden increase in the rate of LN_2 injection into the tunnel circuit.

The total-temperature time histories resulting from the manual-step technique of suddenly changing (i.e., increasing) the rate of LN_2 injection are shown in figures 5 and 6 for initial total temperatures of 278 K and 141 K, respectively. In figure 5(a), the initial manual step occurred at point A when the valve command to the microprocessor, which was in the manual mode, was activated to change the valve setting from 18 percent to 22 percent of full open. After the valves were opened the initial temperature of 278 K decreased rapidly and eventually approached a temperature of about 257 K. At point B, the valve command was reduced to 18 percent and the microprocessor activated. This process resulted in a rapid increase in the temperature. The expanded 15-sec and 3-sec regions are shown in figures 5(b) and 5(c), respectively, with the 0.62-sec circuit time indicated on both figures. Again, as was noted in the auto-ramp method of temperature variation, the manual-step method indicated that while there was an initially steep fall-off, there were no discernible fronts occurring at intervals of the circuit time. The manual-step method was repeated in figure 6 for a lower initial total temperature of 141 K and for a larger change in the valve command. At point A in figure 6(a), the LN_2 valve command to the microprocessor controller was changed from an initial value of 21 percent to 50 percent of full open. There was a sudden decrease in total temperature after the opening of the valves was increased and as the total temperature approached 130 K the valve command was returned to 21 percent at point B. After point B there was a rapid increase in total temperature followed by a more gradual increase toward the original initial temperature. The expanded regions of 15 sec and 3 sec shown in figures 6(b) and 6(c) along with the circuit time of 0.89 sec again indicate clearly that no discernible temperature fronts exist.

The final method of suddenly changing the total temperature in the wind tunnel was accomplished by closing the LN_2 injection valve as shown in figures 7 and 8 for initial total temperatures of 278 K and 134 K, respectively. This was the method used in the ONERA/CERT T'2 wind tunnel to check for temperature fronts. (See fig. 2.) The total pressure for figures 7 and 8 were 2.04 and 3.40 atm,

respectively, and were kept nearly constant with the total-pressure microprocessor in the automatic mode. At point A in figure 7(a), with the total-temperature microprocessor controlled in the manual mode, the LN_2 injection valves were closed from an initial valve command of about 20 percent. After the LN_2 injection valves were closed there was a rapid increase in temperature up to point B at which time the valves were opened to the original valve command of 20 percent. The expanded time scales of 15 sec and 3 sec are shown in figures 7(b) and 7(c), respectively, along with the circuit time of 0.62 sec. It again appears that for the circuit time indicated on the figures, no temperature fronts were present.

The closing of the LN_2 injection valves was repeated at a lower initial total temperature of 134 K and a higher total pressure of 3.40 atm. The results in figure 8(a) show that when the LN_2 injection valves were closed at point A, there was a steady increase in the total temperature. At point B, the valves were reopened to 44 percent which resulted in an initial rapid decrease in total temperature. Again the expanded time scales of 15 and 3 sec are shown in figures 8(b) and 8(c), respectively, with an indicated circuit time of 0.93 sec. As in all the previous figures with an expanded time scale, there were no discernible temperature fronts.

Although some of the data represent a large change in the total temperature with time, with large step changes in the LN_2 flow rate, there appears to be no evidence of temperature fronts existing at intervals of the circuit time in the 0.3-m TCT for the conditions of the present tests; or if they are present, they are of such a small amplitude as to be undetectable with the techniques of this investigation.

The temperature fronts that were predicted by Tripp to exist in the 0.3-m TCT in reference 1 (fig. 1) were not found in the results of this test. The reason temperature fronts were predicted from numerical results, in reference 1, but not found experimentally, can possibly be attributed to two areas in Tripp's mathematical model which did not properly account for two of the complex flow mechanisms that exist in the 0.3-m TCT: (1) the dynamics of the heat transfer between the gas and the tunnel liner and (2) the mixing dynamics in the tunnel circuit and particularly in the region of the fan.

The temperature fronts that were observed in the ONERA/CERT T'2 injection driven wind tunnel (see fig. 2 and ref. 2) could almost be expected because of the internal insulation which greatly reduced the heat transfer at the tunnel liner. In addition, after the LN_2 supply was cut off, the injectors continued to supply 273 K air to the tunnel at a rate nearly equal to the LN_2 injection rate. The injection of the relatively warm air undoubtably initially contributed to the existence of the temperature fronts for one or two circuit times. (See fig. 2.) Beyond about two circuit times, the mixing associated with the ejector operation caused the temperature fronts to decay and produce a more uniform temperature increase as can be seen in figure 2.

Velocity and Pressure Fluctuations

Results of measurements of velocity and pressure fluctuations, made prior to the temperature-front investigation using a hot-wire probe and a dynamic pressure transducer, are presented in figures 9 through 12. For the fluctuating measurements the mean tunnel flow was in a steady-state condition (i.e., Mach number, total temperature, and total pressure were constant with time). The velocity fluctuations, normalized by the local mean velocity, shown in figure 9 (T_t = 280 K) were about 2 percent over the test range of Mach number and Reynolds number. At T_t = 140 K,

the normalized fluctuations (fig. 10) increased slightly both with Mach number and Reynolds number and ranged from 1.8 to 3.0 percent.

The rms pressure fluctuations measured at the wall, normalized by the local mean static pressure in figure 11 (T_t = 280 K), range from about 2×10^{-4} to 2×10^{-3} or 0.02 to 0.20 percent. The levels in figure 11 show a significant increase with increasing Mach number and for a constant Mach number show a slight decrease with Reynolds number. When the total temperature was decreased from 280 K to 140 K, with the corresponding significant increase in Reynolds number, there was only a small increase in the levels of the pressure fluctuations for the various Mach numbers. (See fig. 12.) The variation of the pressure fluctuations with Mach number and Reynolds number shown in figure 12 is approximately the same as that found for the higher temperature in figure 11.

Once some assumptions are made, velocity fluctuations in the settling chamber can be calculated from measured pressure fluctuations by using the simple wave equation

$$\frac{\tilde{u}}{\bar{u}} = \frac{1}{\gamma M_{sc}} \frac{\tilde{p}}{\bar{p}}$$

The results show the velocity fluctuations calculated from pressure fluctuations range from about 36 to 113 percent of the velocity fluctuations measured with a hot wire, for test-section Mach numbers of 0.3 to 0.8, respectively. These results indicate as the test-section Mach number increases to the range used in transonic testing, the velocity fluctuations in the settling chamber are primarily due to sound.

Fluctuating Pressure and Velocity Power Spectra

The measurements from the pressure transducer and hot wire were used to obtain power spectra for the normalized pressure and velocity fluctuations. The results for the fluctuating pressure spectra are presented in figures 13 and 14 and the fluctuating velocity spectra in figures 15 and 16. There are significant discrete frequencies present in the spectra and they are most evident in the spectra obtained with the pressure transducer. (See figs. 13 and 14.) The discrete frequencies were apparently generated by the fundamental of the fan blade passing frequency and its harmonics. A three-dimensional plot of the fluctuating pressure spectra versus frequency is shown in figure 13 for Mach numbers of 0.30, 0.50, 0.60, 0.70, and 0.80 and show numerous discrete spikes in the spectra apparently resulting from the fan blade passage. The level of the spectra shows a slight increase with increasing Mach number at the low frequencies and a more significant increase in level at the higher frequencies. The spectra in figure 14 are shown for the frequency nondimensionalized by the rotational speed of the fan n and the number of blades on the fan N. The data correlate quite well for the fundamental frequency and the first eight harmonics by using this dimensionless frequency parameter over a range of Mach number from 0.30 to 0.80. These results corroborate the indications from figure 13 which indicated the peaks in the pressure spectra are from the fan blade passage.

The spectra for the velocity fluctuations, obtained with the hot wire in the settling chamber, have been transformed into dimensionless coordinates and are shown for a range of Mach numbers in figures 15 and 16. The frequency has been nondimensionalized by the velocity in the settling chamber and the diameter of the settling

chamber. The discrete peaks from the fan blade passage are not discernible at frequencies higher than about the third or fourth harmonic of the fan blade passage because the random velocity fluctuations mask the discrete frequencies of the fan blade at the higher frequencies. In figures 13 and 14 there are discrete frequencies evident up to the eighth harmonic of the fan blade passage because the pressure transducer responds primarily to the pressure pulse; however, in figures 15 and 16 the data become random after the third or fourth harmonic because the hot wire responds to both the pressure fluctuation and the vorticity in the flow. There are large discrete frequencies (i.e., spikes) in the spectra in figure 15 that occur between $3 \times 10^3 < \frac{2\pi D}{u} f < 1 \times 10^4$ for each of the Mach numbers at $T_t = 140$ K. The reason for these spikes is unknown; however, it is speculated these discrete frequencies could possibly be due to four causes.

One possible cause of these spikes is eddy shedding behind the screens in the settling chamber similar to the eddy shedding noticed by Schubauer, Spangenberg, and Klebanoff (ref. 9). In the test setup in the 0.3-m TCT the hot wire was located 7.75 in. downstream of the 40-mesh screen, which had a solidity of 0.452. The Reynolds number based on the diameter of the screen wire (0.0065 in.) was well above the critical Reynolds number required for eddy shedding; however, as the Mach number was increased from 0.30 to 0.80 the frequency at which the spikes occurred (about 8 kHz) remained constant. This constant frequency is unlike the results reported in reference 9 and may be due in part to the much higher Reynolds number (based on the diameter of the screen wire) than those reported in reference 9.

Another possibility for the large spikes noted in figure 15 could be a vortex shedding from the hot wire itself. The Reynolds numbers based on the hot-wire diameter range from 42 to 81 which are in the range of flow condition where the "Von Karman vortex-streets" could be observed; however, Strouhal numbers for the hot wire were about two orders of magnitude below classical Strouhal numbers presented by Roshko (ref. 10).

A third cause of the spikes could be leaks in the settling chamber which could generate noise that might be detected in the settling chamber. This source must be discounted since the spikes did not show up in the spectra from the pressure transducer.

A fourth cause of the spikes could be "strain gauging" of the hot wire. The spikes occurred at a constant frequency and increased in level with Mach numbers which suggests strain gauging. However, the low velocities and low loading of the wire cast doubt to this argument. There were no discrete frequencies in the hot-wire spectra at 280 K, shown in figure 16, even though the wire was mounted on the probe with little or no slack. However, it is possible for the wire to contract enough at 140 K to become taut, and under this condition it might be possible to excite the taut wire causing it to vibrate even with a low loading. If this is true, to avoid strain gauging, slack must be put in the hot wires when testing at cryogenic temperatures even though the flow velocity is very low.

A review of these four possible causes for the spikes in the nondimensional spectra (fig. 15) indicates that none of the explanations provides a completely satisfactory answer, and the reason for the spikes is still uncertain.

Liquid Nitrogen Particles in Tunnel Flow

There has been much conjecture about the presence of liquid nitrogen droplets in the flow medium throughout the circuit of the 0.3-m TCT. Results presented by Singh, Marple, and Davis (ref. 11) indicated that no LN_2 droplets were observed in the 0.3-m TCT at temperatures slightly higher than the free-stream saturation values (a total temperature of about 100 K) at the highest total pressure. Recent results of Hall (ref. 12) corroborated the work of Singh, Marple, and Davis (ref. 11), using a different measuring technique. Hall found that for a steady-state flow condition, there were an insignificant number of liquid droplets in the test medium in the 0.3-m TCT above about $T_t = 100$ K (i.e., slightly above free-stream saturation temperature). However, the point of conjecture arises from earlier tests by Gartrell, Gooderum, Hunter, and Meyers (ref. 13) which indicated that LN_2 droplets existed in the 0.3-m TCT up to a total temperature of 250 K based on the number of particles they found from velocity measurements by using a laser Doppler velocimeter. Because of the conflicting results on the existence of LN_2 droplets at various total temperatures in the 0.3-m TCT, the present data included an analysis to further investigate the possible existence of LN_2 droplets in steady-state flows.

This analysis was based on a statistical technique which uses the skewness parameter of the normalized velocity fluctuations to infer the existence (or nonexistence) of LN_2 droplets. The skewness is defined as the third central moment of the random variable, and if it is equal to zero, the probability distribution is symmetric about the mean. First, the skewness of the pressure fluctuations was calculated from

$$\text{Skewness}\left(\frac{\tilde{p}}{\bar{p}}\right)_{sc} = \int_{-\infty}^{\infty}\left(\frac{\tilde{p}}{\bar{p}}\right)^3 P\left(\frac{\tilde{p}}{\bar{p}}\right) d\,\frac{\tilde{p}}{\bar{p}}$$

to determine whether the disturbances in the settling chamber were symmetric. (See fig. 17.) It can be inferred from figure 17 that the probability distribution of the pressure fluctuations (from a pressure transducer) are symmetrical since the values of skewness scatter nearly uniformly above and below zero (i.e., values close to zero) over the test range of Mach number and Reynolds number. Based on the results of figure 17, it was postulated that skewness of the normalized velocity fluctuations (from a hot wire) should also scatter uniformly about and close to zero unless LN_2 droplets were striking the hot wire. If droplets were to strike the hot wire, they would cause the instantaneous voltage to increase and result in a positive skewness. The skewness of the normalized velocity fluctuations was calculated from

$$\text{Skewness}\left(\frac{\tilde{u}}{\bar{u}}\right)_{sc} = \int_{-\infty}^{\infty}\left(\frac{\tilde{u}}{\bar{u}}\right)^3 P\left(\frac{\tilde{u}}{\bar{u}}\right) d\,\frac{\tilde{u}}{\bar{u}}$$

(see fig. 18) and shows a negative skewness. This negative skewness indicates there was not a significant number of liquid droplets striking the hot wire. In fact, the negative skewness would indicate the existence of solid particles striking the hot wire (i.e., due to energy addition to the wire), a result also reported by Hall in reference 12, which he attributed the solid particles at temperatures below 200 K to frozen oil droplets. Thus, from the skewness parameter developed from the normalized

fluctuating velocities (fig. 18), it appears that over a large range of Mach number and Reynolds number, down to a total temperature of 140 K, there are no significant number of LN_2 droplets in the steady-state mean flow, but there could be solid particles in the flow. The results from this study and the results from Hall (ref. 12) indicated the particles in the laser Doppler velocimeter (LDV) experiment of Gartrell, Gooderum, Hunter, and Meyers (ref. 13) were probably solid particles, of possibly oil or some other impurity, and not LN_2 droplets.

CONCLUSIONS

From measurements made in the settling chamber of the Langley 0.3-m TCT over a range of Mach number, Reynolds number, and total temperature with a hot-wire probe and a pressure transducer, the following conclusions can be made:

(1) There were no indications of the existence of temperature fronts based on temperatures measured with a high-response hot-wire probe using three different techniques to obtain significant step changes in the rate of LN_2 injection.

(2) The normalized pressure and velocity fluctuations at two total temperatures and over a large range of Mach number and Reynolds number were about 0.02 to 0.20 percent and about 1.8 to 3.0 percent, respectively.

(3) The pressure fluctuation power spectra from a pressure transducer correlate with the fan blade passage through the eighth harmonic of the fundamental frequency.

(4) The velocity fluctuation power spectra from hot-wire data do not indicate peaks due to the fan blade passage beyond about the third or fourth harmonic because of the higher levels and random nature of the velocity fluctuations at the higher frequencies.

(5) The cause of the spikes that occurred in the nondimensional spectra of the velocity fluctuations, at a total temperature of 140 K, is uncertain.

(6) Down to a total temperature of 140 K, there was no evidence of liquid nitrogen droplets in the flow based on an analysis of the skewness of the fluctuating pressure and velocity signal.

NASA Langley Research Center
Hampton, VA 23665-5225
March 17, 1986

REFERENCES

1. Tripp, John S.: Development of a Distributed-Parameter Mathematical Model for Simulation of Cryogenic Wind Tunnels. NASA TP-2177, 1983.

2. Blanchard, A.; and Dor, J. B.: Essais Dynamiques Effectues dans la Soufflerie Cryogenique T'2 Resultant d'une Variation de l'Injection d'Azote Liquide (Dynamic Tests Performed in the Cryogenic T'2 Wind Tunnel Resulting From Changes in the Injection [Rate] of the Liquid Nitrogen). CRF 5007 AYD, ONERA/CERT, Apr. 1979.

3. Kilgore, Robert A.: Design Features and Operational Characteristics of the Langley 0.3-Meter Transonic Cryogenic Tunnel. NASA TN D-8304, 1976.

4. Ray, Edward J.; Ladson, Charles L.; Adcock, Jerry B.; Lawing, Pierce L.; and Hall, Robert M.: Review of Design and Operational Characteristics of the 0.3-Meter Transonic Cryogenic Tunnel. NASA TM-80123, 1979.

5. Kilgore, Robert A.: Experience in the Control of a Continuous Flow Cryogenic Tunnel. Cryogenic Wind Tunnels, AGARD-LS-111, May 1980, pp. 14-1 - 14-15.

6. Balakrishna, S.: Synthesis of a Control Model for a Liquid Nitrogen Cooled, Closed Circuit, Cryogenic Nitrogen Wind Tunnel and Its Validation. NASA CR-162508, 1980.

7. Thibodeaux, Jerry J.; and Balakrishna, S.: Development and Validation of a Hybrid-Computer Simulator for a Transonic Cryogenic Wind Tunnel. NASA TP-1695, 1980.

8. Kovásznay, Leslie S. G.: Turbulence in Supersonic Flow. J. Aeronaut. Sci., vol. 20, no. 10, Oct. 1953, pp. 657-674, 682.

9. Schubauer, G. B.; Spangenberg, W. G.; and Klebanoff, P. S.: Aerodynamic Characteristics of Damping Screens. NACA TN 2001, 1950.

10. Roshko, Anatol: On the Development of Turbulent Wakes From Vortex Streets. NACA Rep. 1191, 1954. (Supersedes NACA TN 2913.)

11. Singh, Jag J.; Marple, Charles G.; and Davis, William T.: Characterization of Particles in the Langley 0.3-Meter Transonic Cryogenic Tunnel Using Hot Wire Anemometry. NASA TM-84551, 1982.

12. Hall, Robert M.: Pre-Existing Seed Particles and the Onset of Condensation in Cryogenic Wind Tunnels. AIAA-84-0244, Jan. 1984.

13. Gartrell, Luther R.; Gooderum, Paul B.; Hunter, William W., Jr.; and Meyers, James F.: Laser Velocimetry Technique Applied to the Langley 0.3-Meter Transonic Cryogenic Tunnel. NASA TM-81913, 1981.

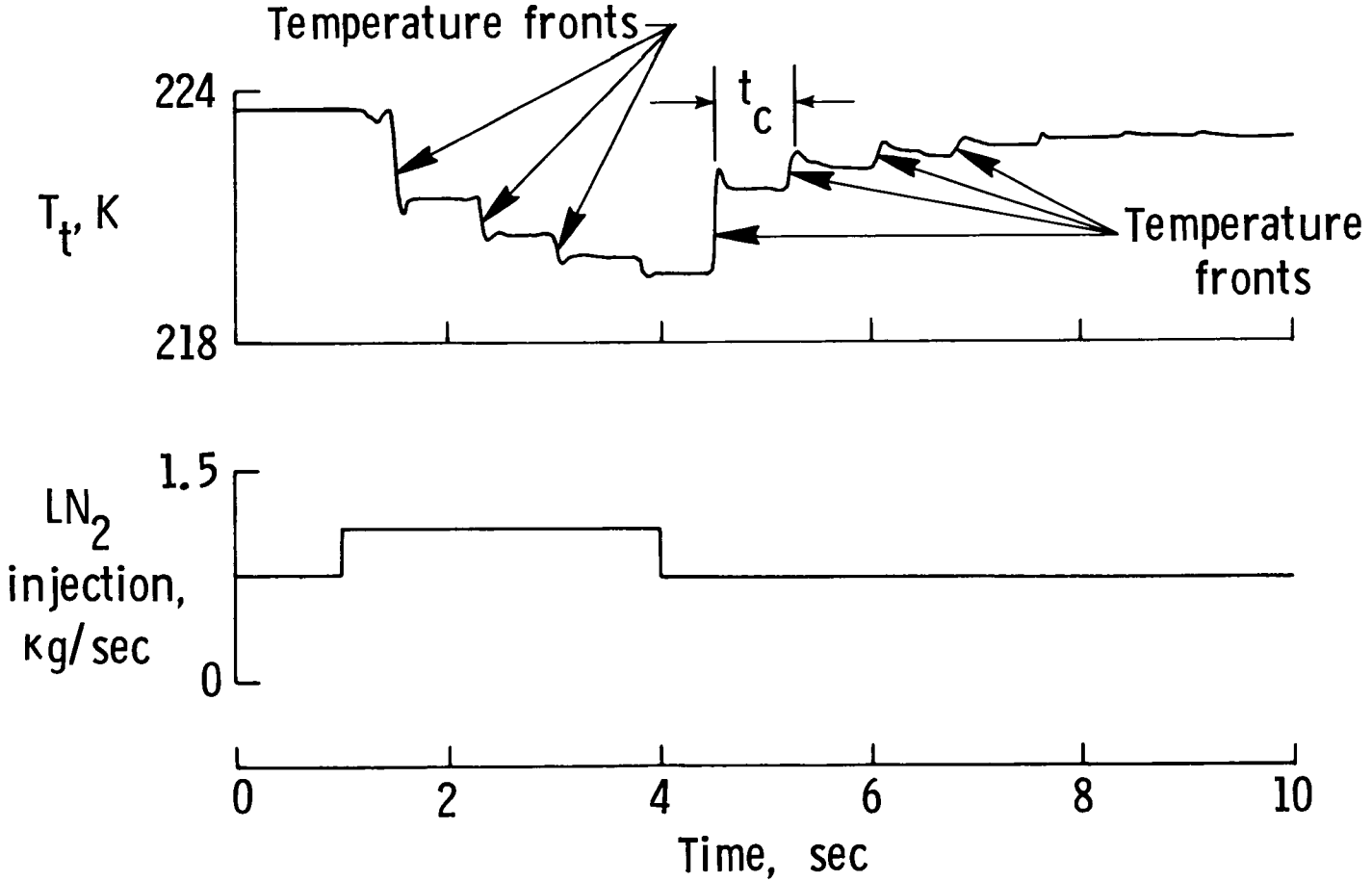

Figure 1.- Temperature fronts predicted in 0.3-m TCT from calculations of Tripp (ref. 1) based on mathematical model for simulation of flow. $t_c \approx 0.7$; $M_\infty \approx 0.67$; $T_t \approx 224$ K; $p_t = 2.1$ atm.

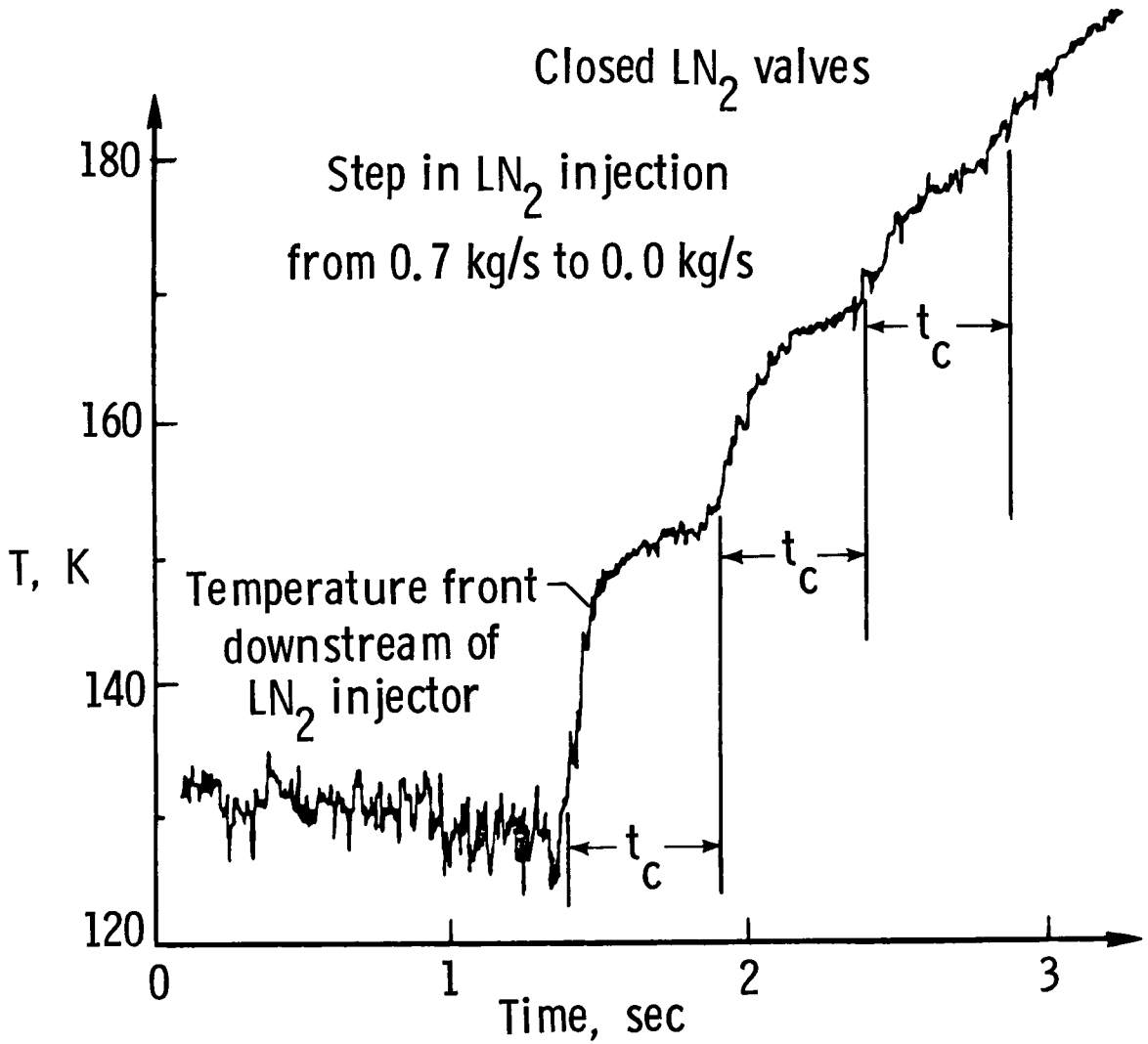

Figure 2.- Temperature fronts measured in the ONERA/CERT T'2 cryogenic wind tunnel (ref. 2).

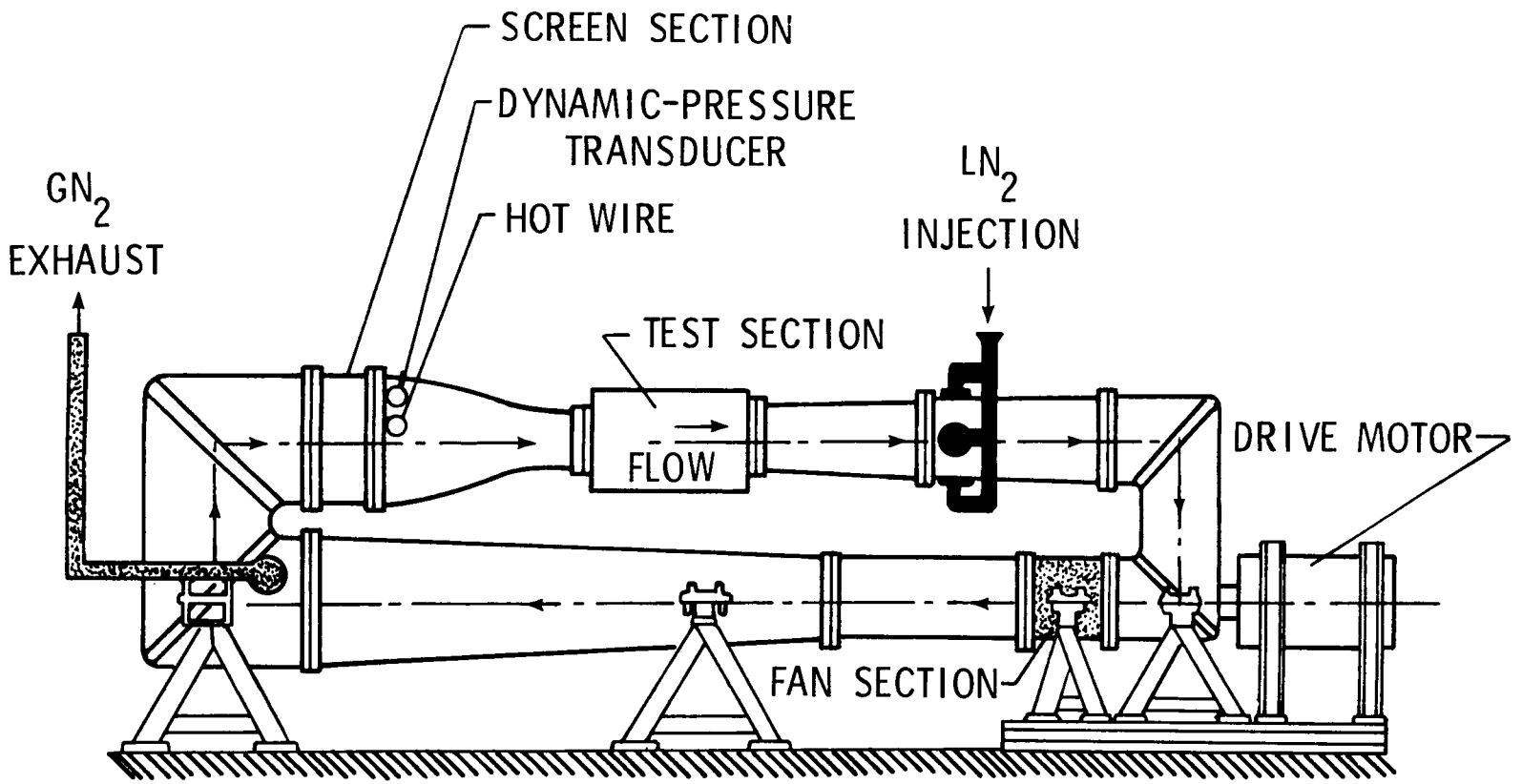

(a) Dynamic instrumentation in settling chamber.

Figure 3.- Schematic of Langley 0.3-Meter Transonic Cryogenic Tunnel.

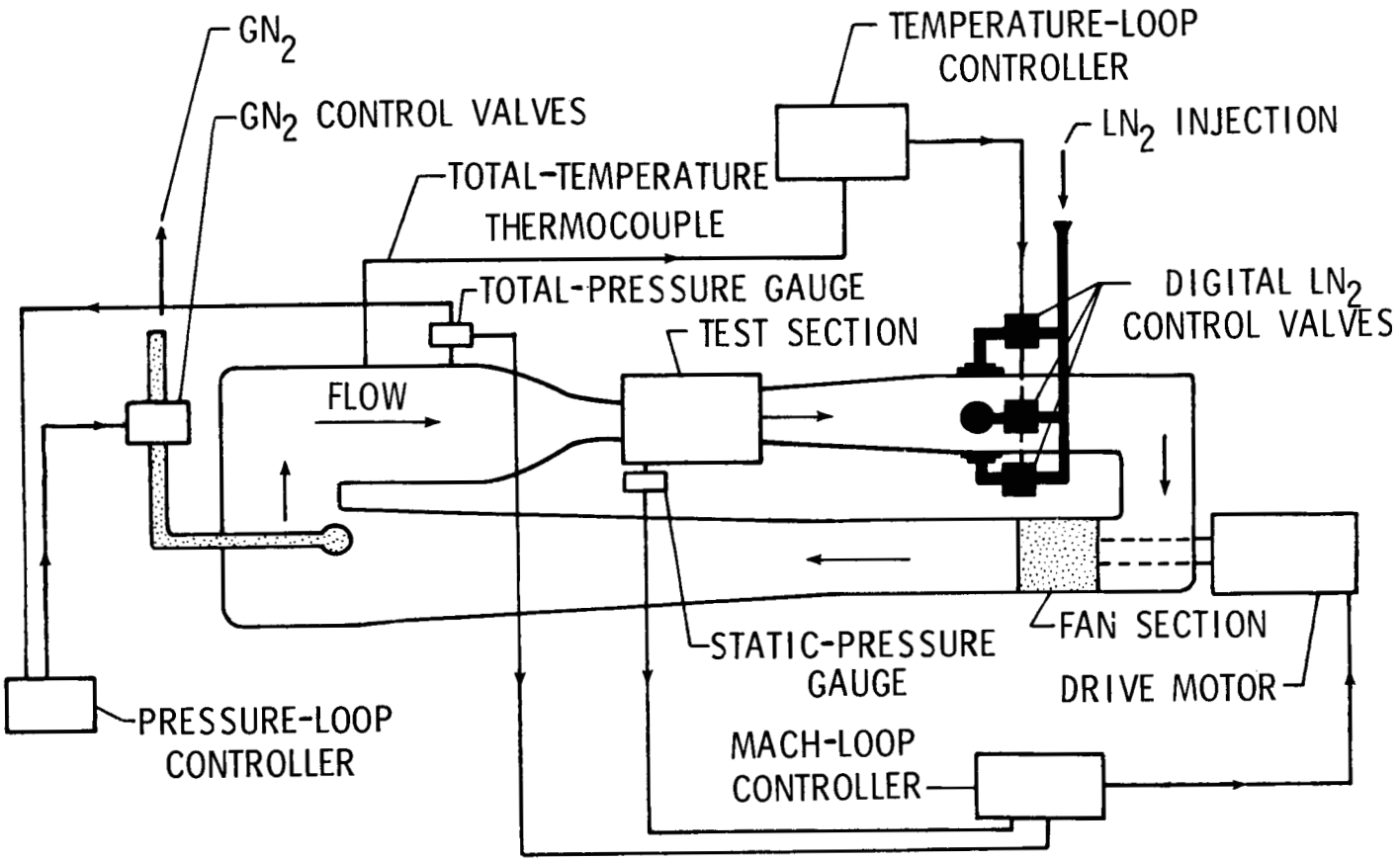

(b) Control system.

Figure 3.- Concluded.

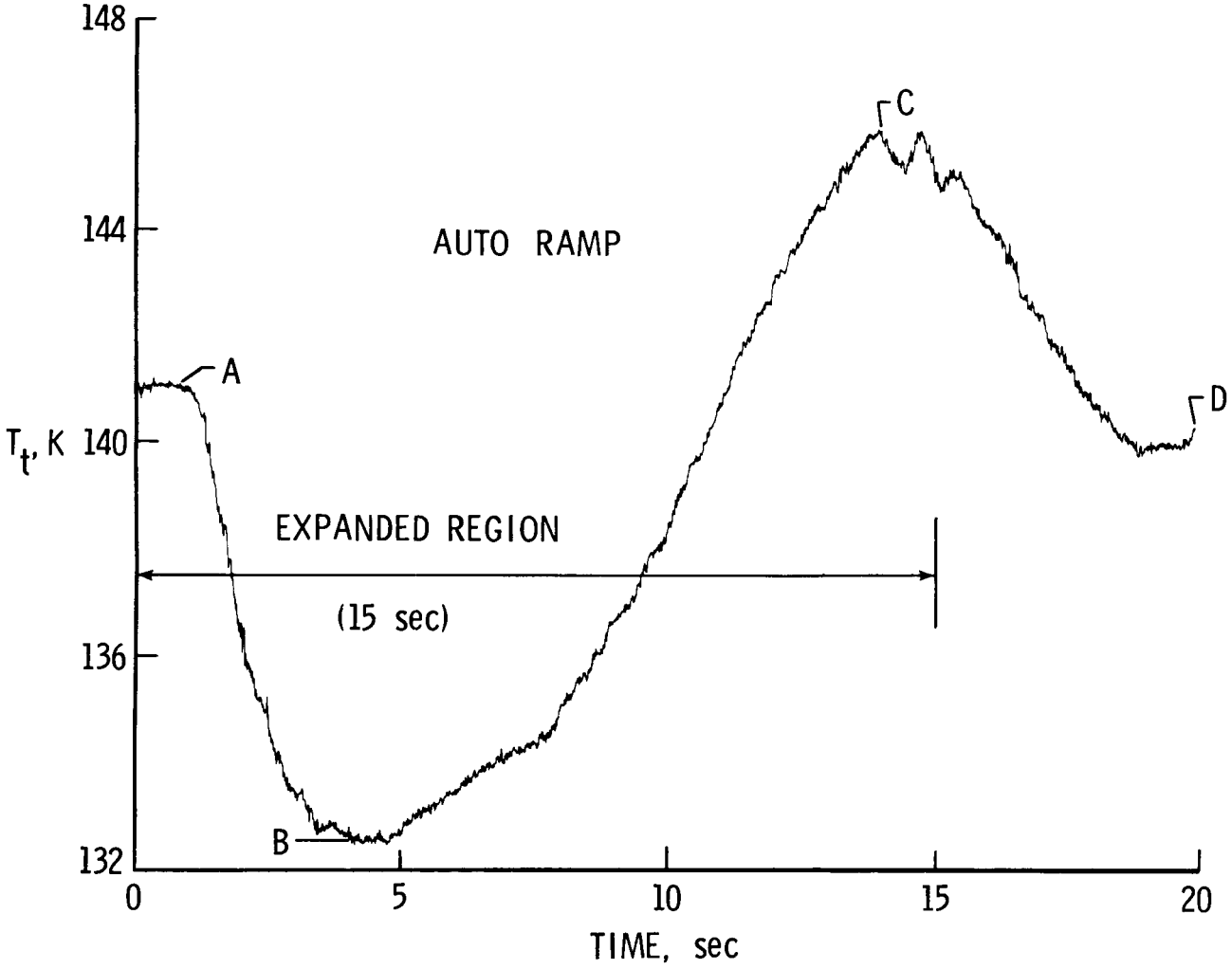

(a) Complete time history.

Figure 4.- Variation of settling chamber total temperature for $M_\infty = 0.70$, $p_t = 2.04$ atm, $T_{t,i} \approx 141$ K, and $R_\infty = 22.5 \times 10^6$.

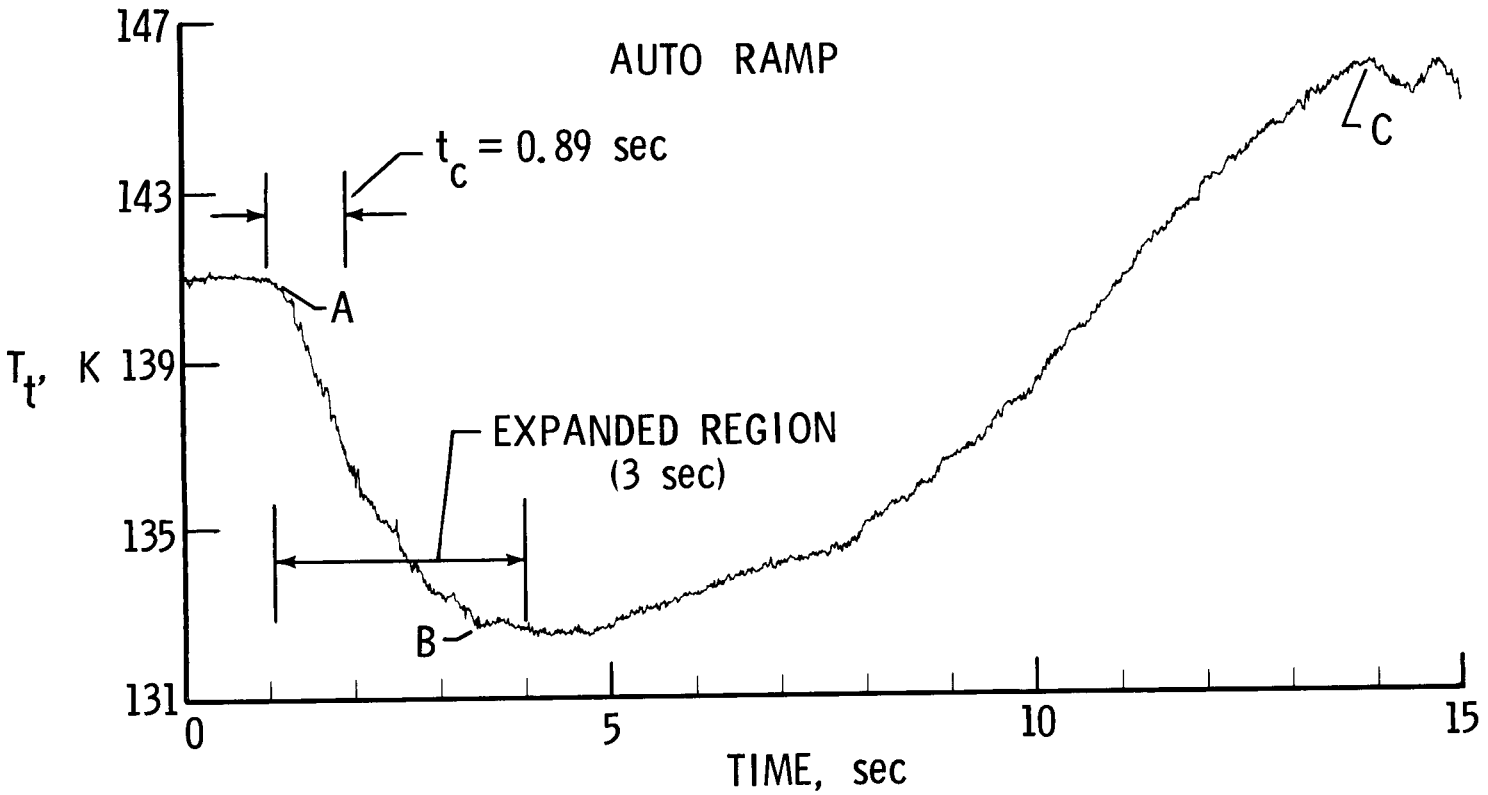

(b) 15-sec expanded region.

Figure 4.- Continued.

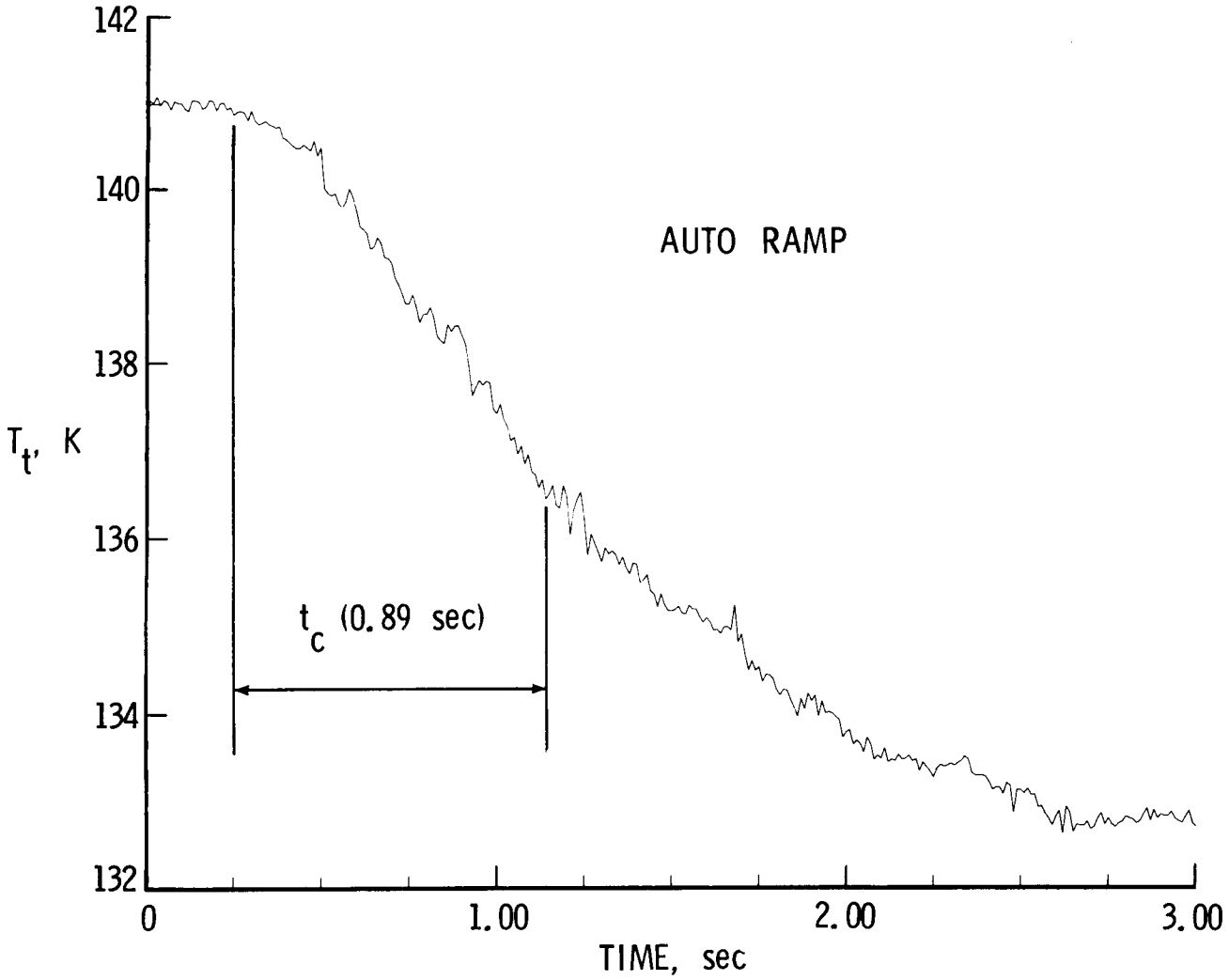

(c) 3-sec expanded region.

Figure 4.- Concluded.

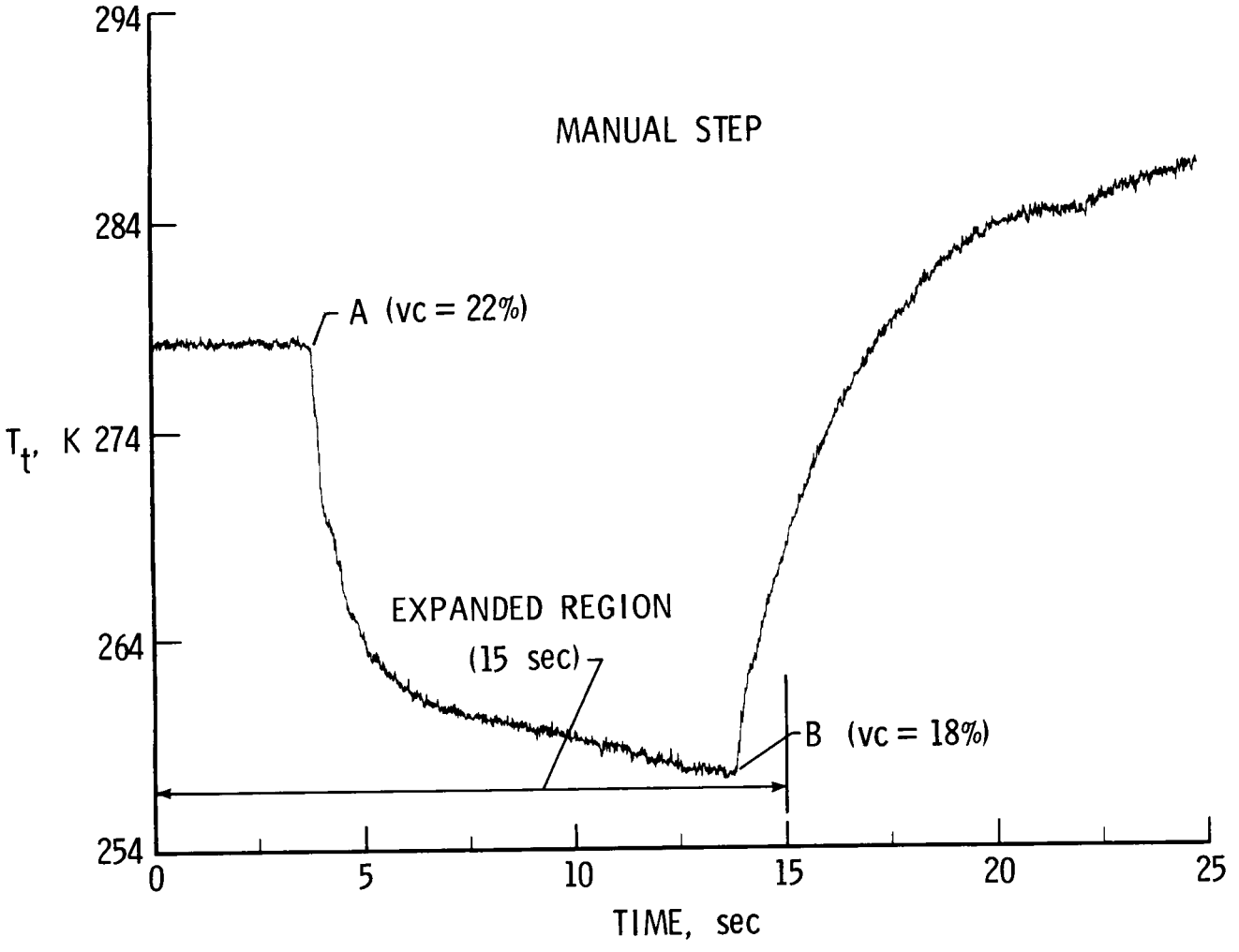

(a) Complete time history.

Figure 5.- Variation of settling chamber total temperature for $M_\infty = 0.70$, $p_t = 2.04$ atm, $T_{t,i} \approx 278$ K, and $R_\infty = 8.6 \times 10^6$.

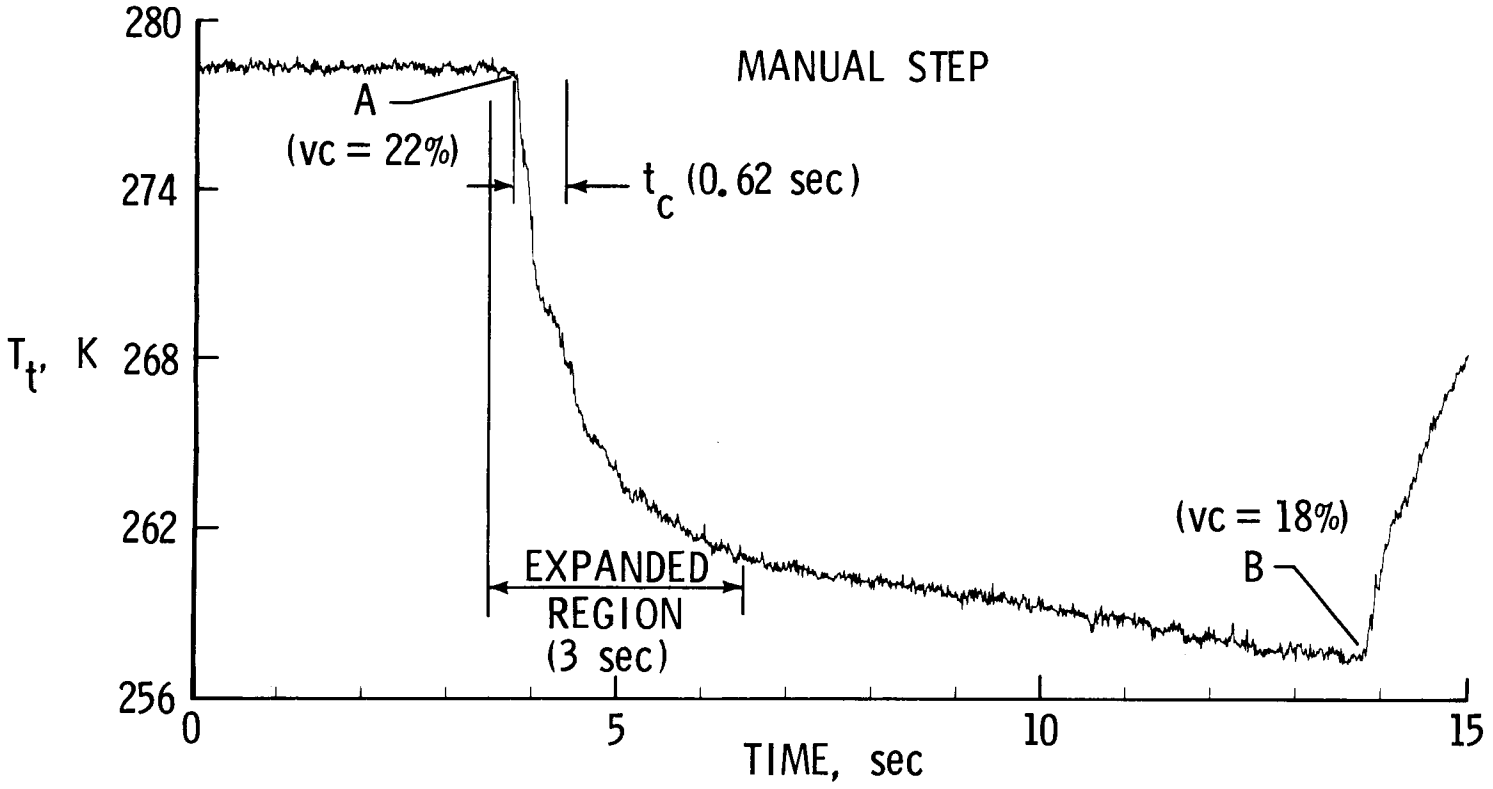

(b) 15-sec expanded region.

Figure 5.- Continued.

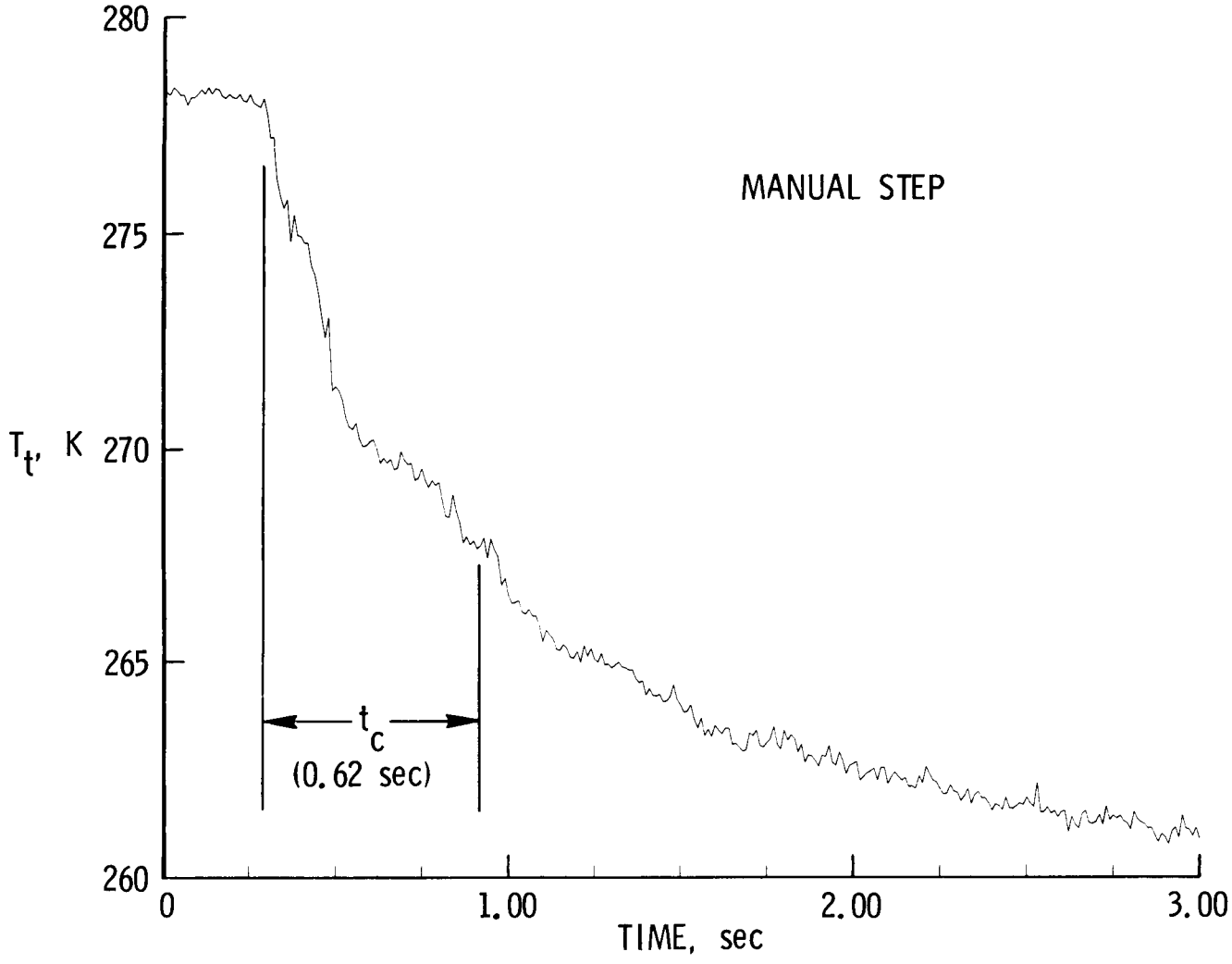

(c) 3-sec expanded region.

Figure 5.- Concluded.

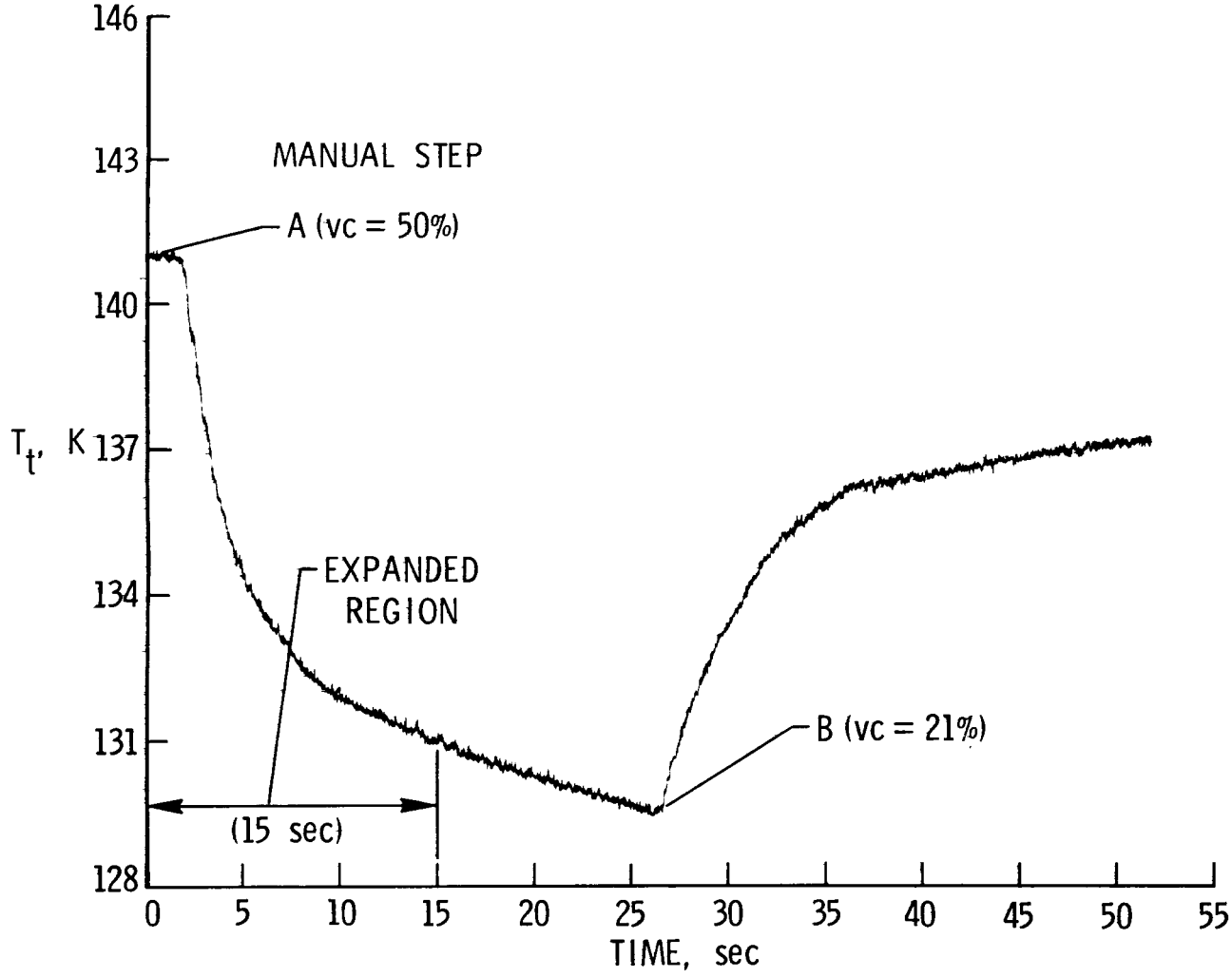

(a) Complete time history.

Figure 6.- Variation of settling chamber total temperature for $M_\infty = 0.70$, $p_t = 2.04$ atm, $T_{t,i} \approx 141$ K, and $R_\infty = 8.6 \times 10^6$.

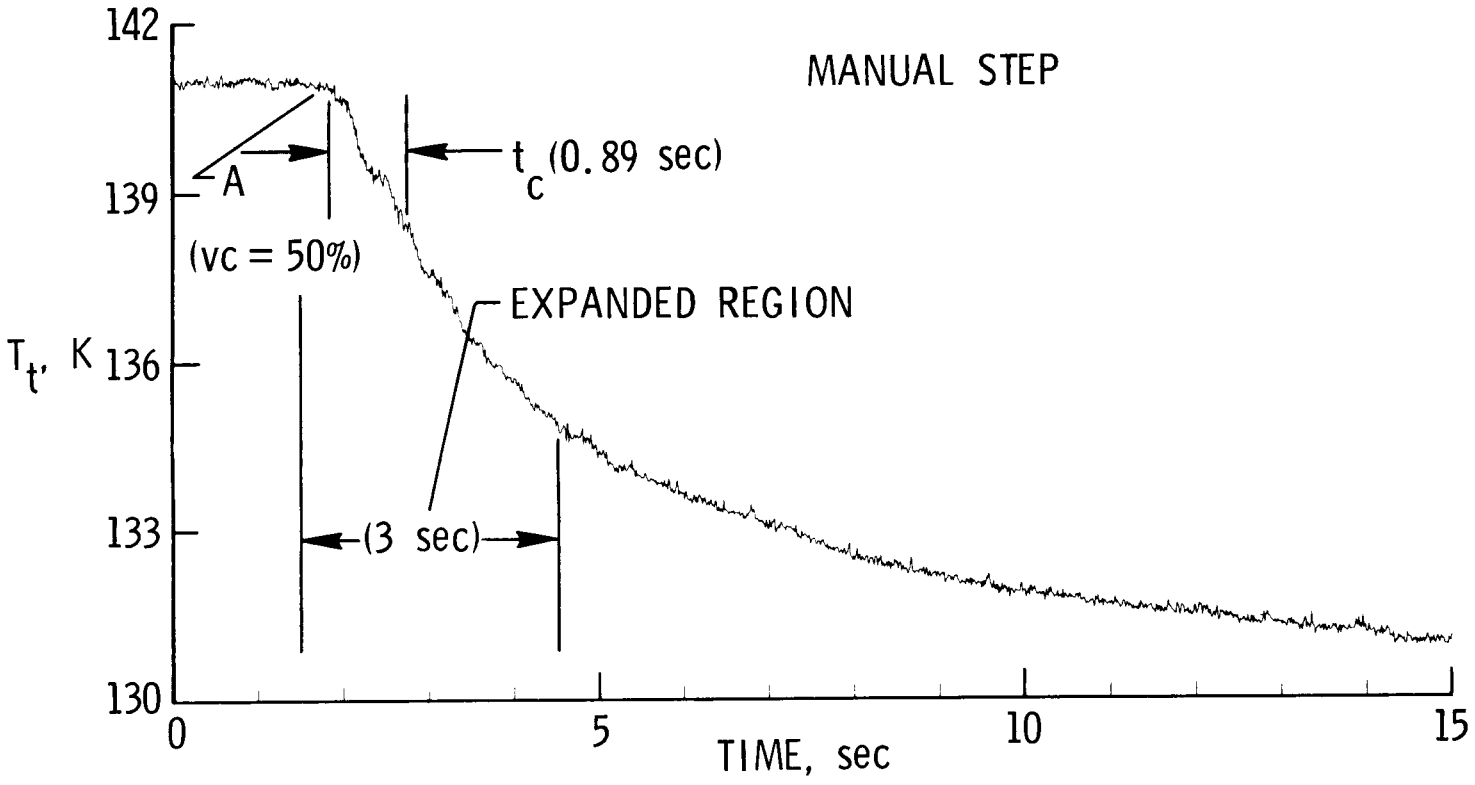

(b) 15-sec expanded region.

Figure 6.- Continued.

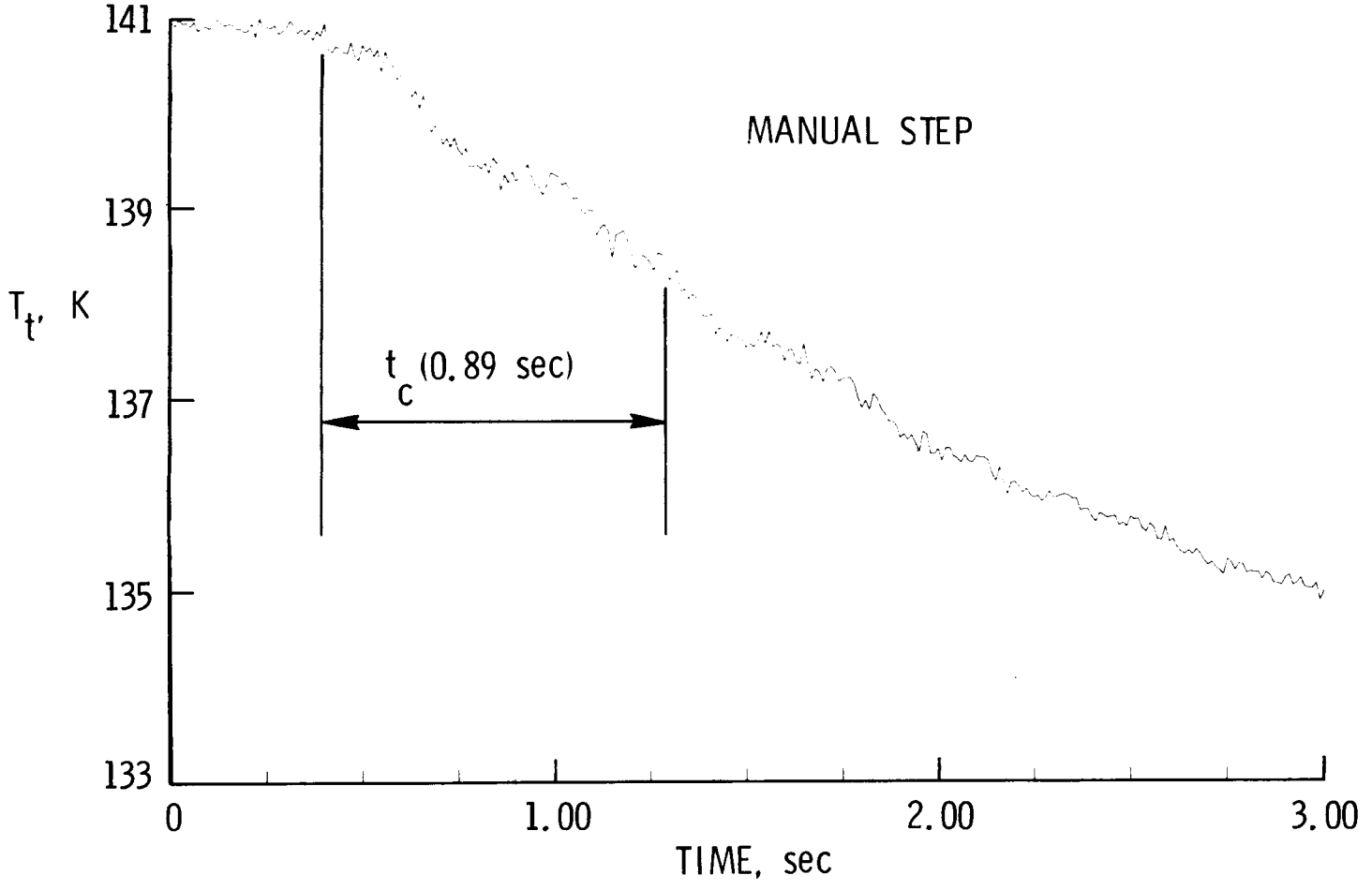

(c) 3-sec expanded region.

Figure 6.- Concluded.

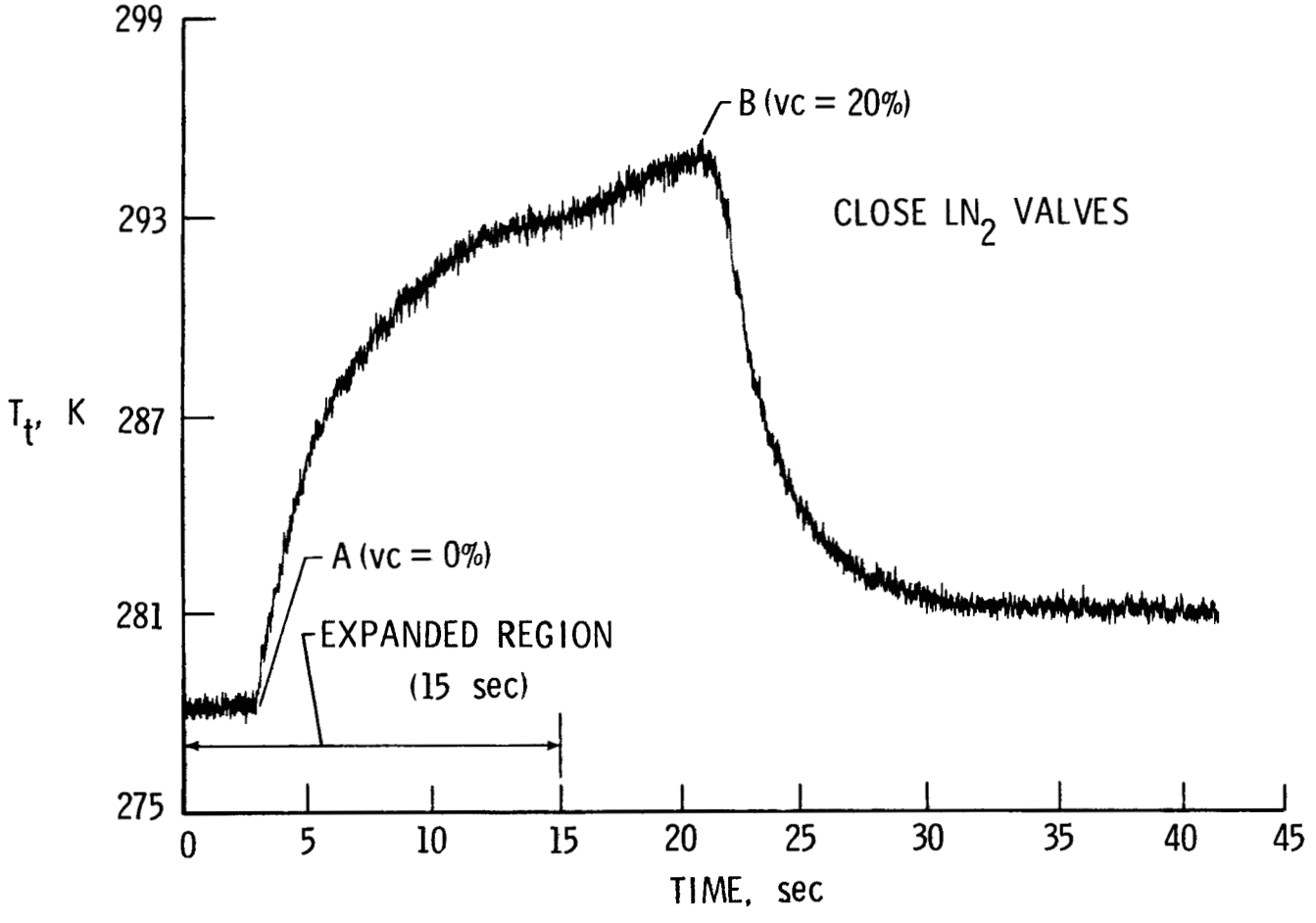

(a) Complete time history.

Figure 7.- Variation of settling chamber total temperature for $M_\infty = 0.70$, $p_t = 2.04$ atm, $T_{t,i} \approx 278$ K, and $R_\infty = 8.6 \times 10^6$.

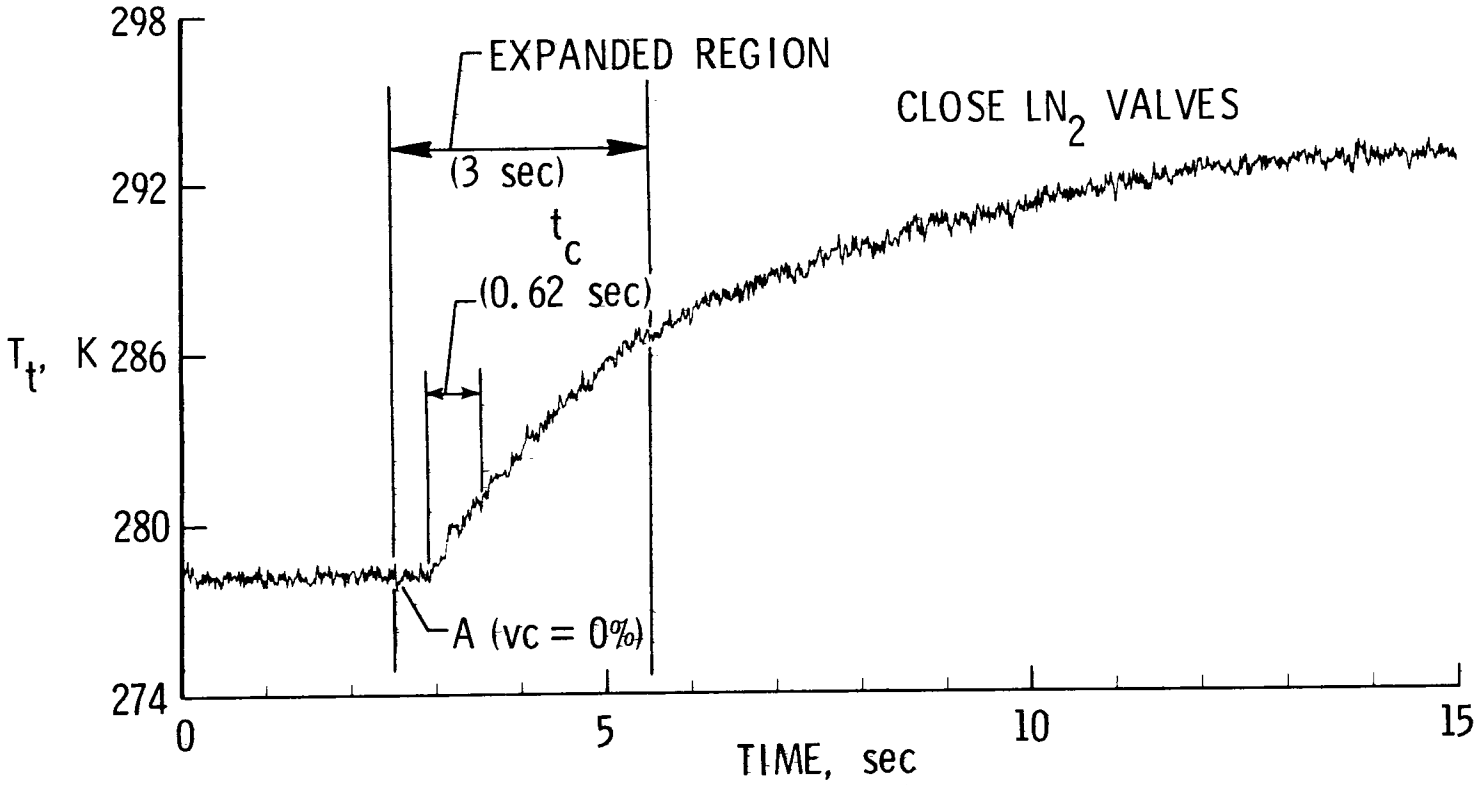

(b) 15-sec expanded region.

Figure 7.- Continued.

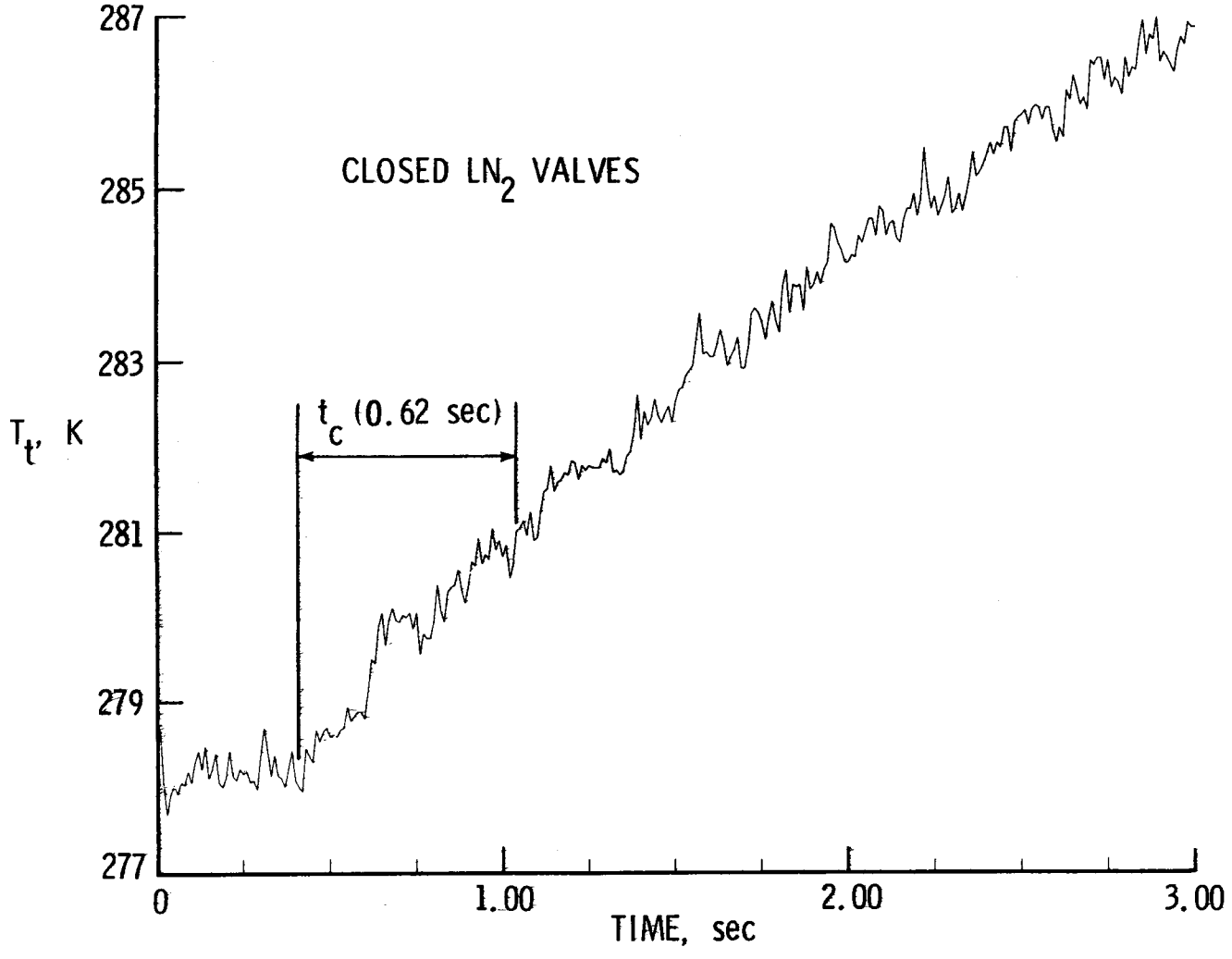

(c) 3-sec expanded region.

Figure 7.- Concluded.

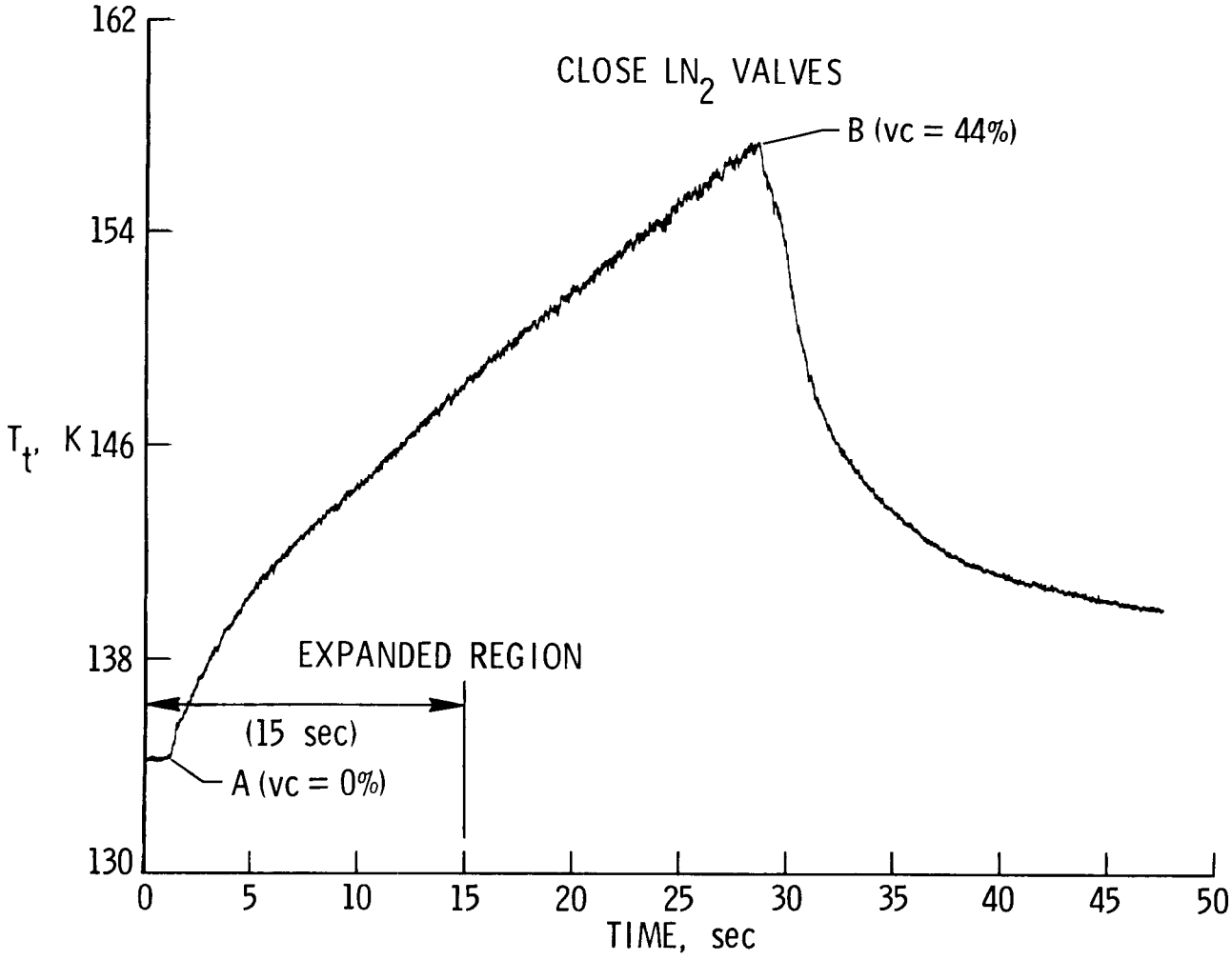

(a) Complete time history.

Figure 8.- Variation of settling chamber total temperature for $M_\infty = 0.70$, $p_t = 3.40$ atm, $T_{t,i} \approx 134$ K, and $R_\infty = 37.5 \times 10^6$.

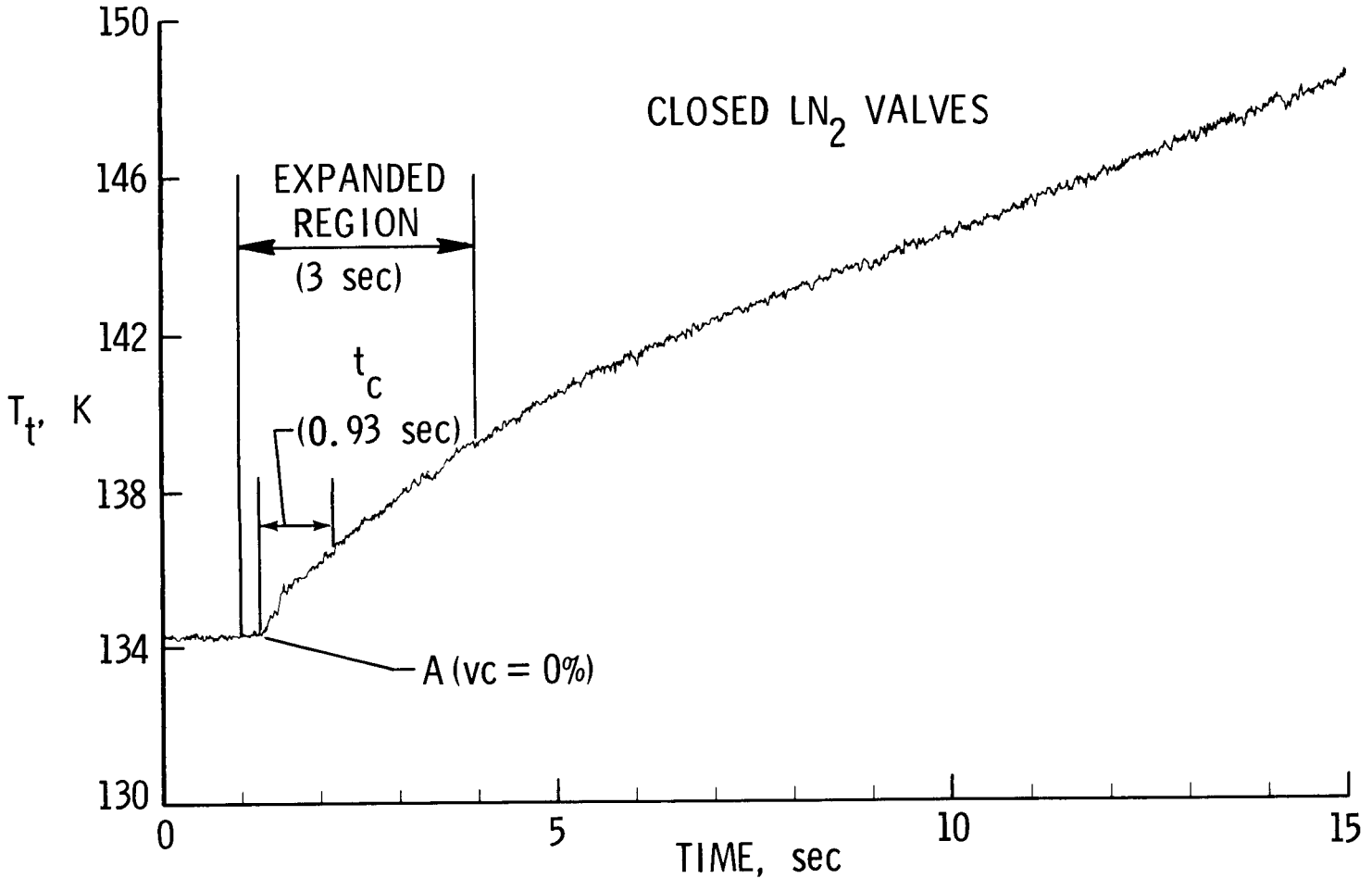

(b) 15-sec expanded region.

Figure 8.- Continued.

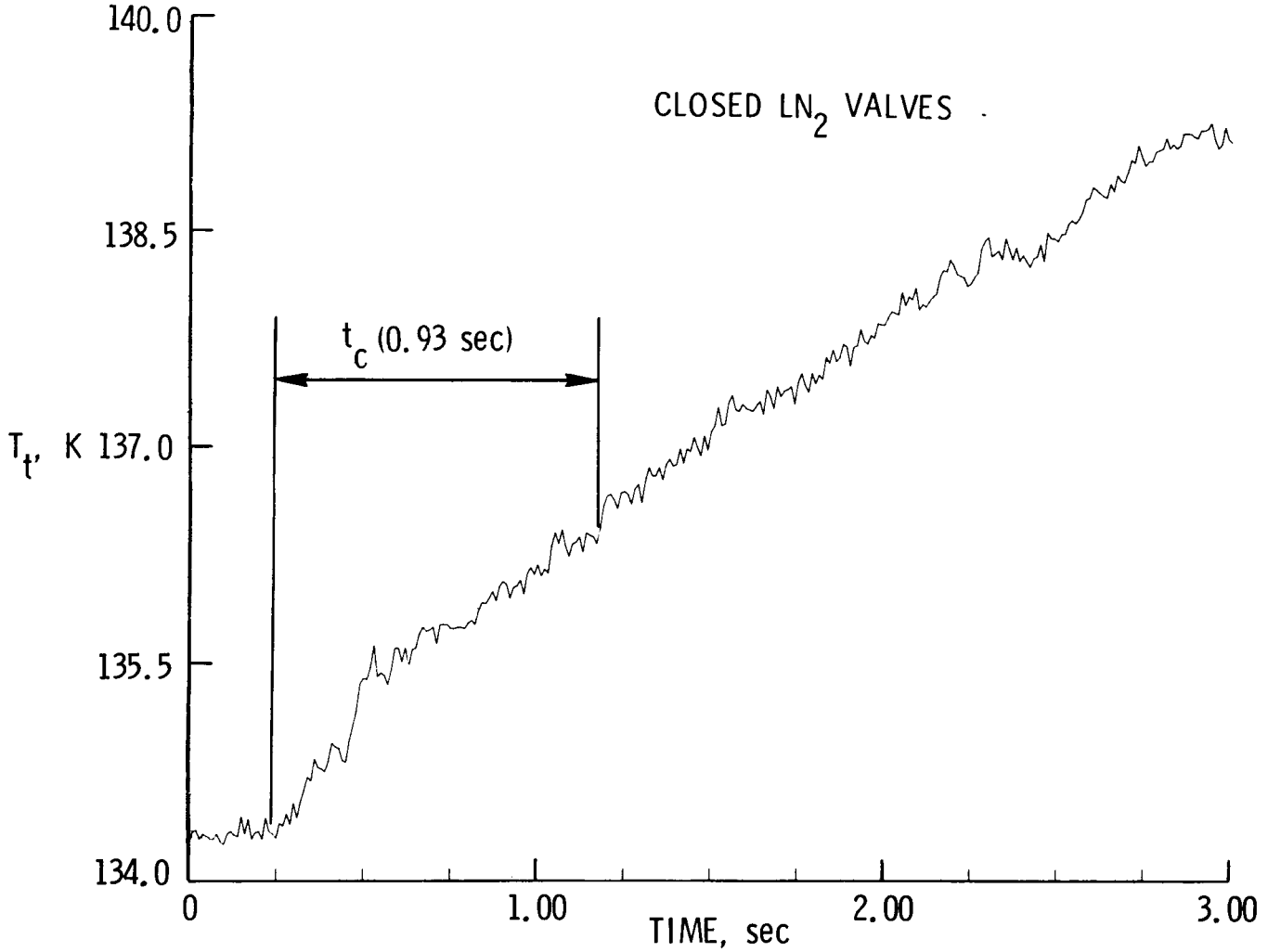

(c) 3-sec expanded region.

Figure 8.- Concluded.

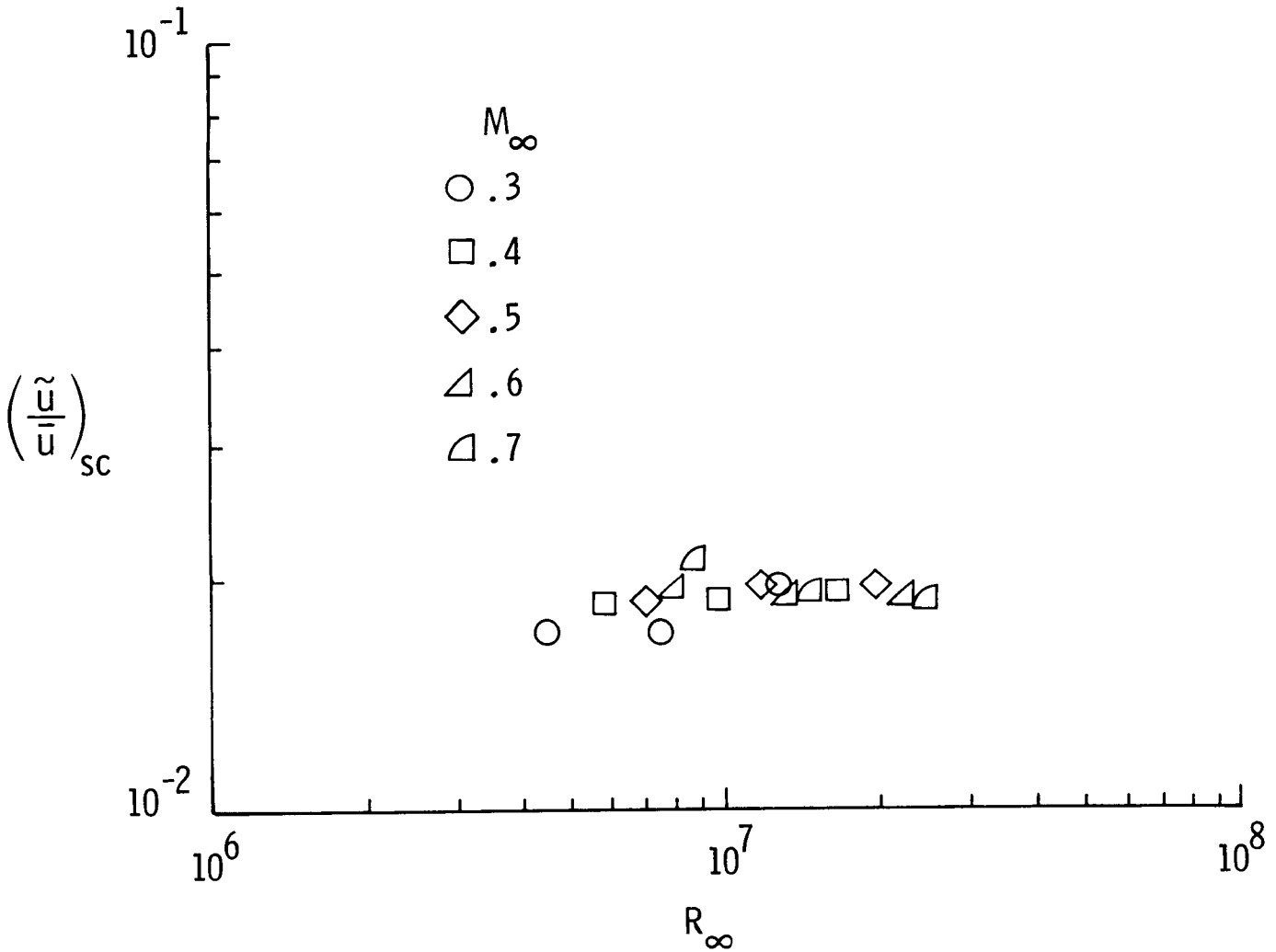

Figure 9.- Velocity fluctuation in settling chamber at near ambient conditions. T_t = 280 K.

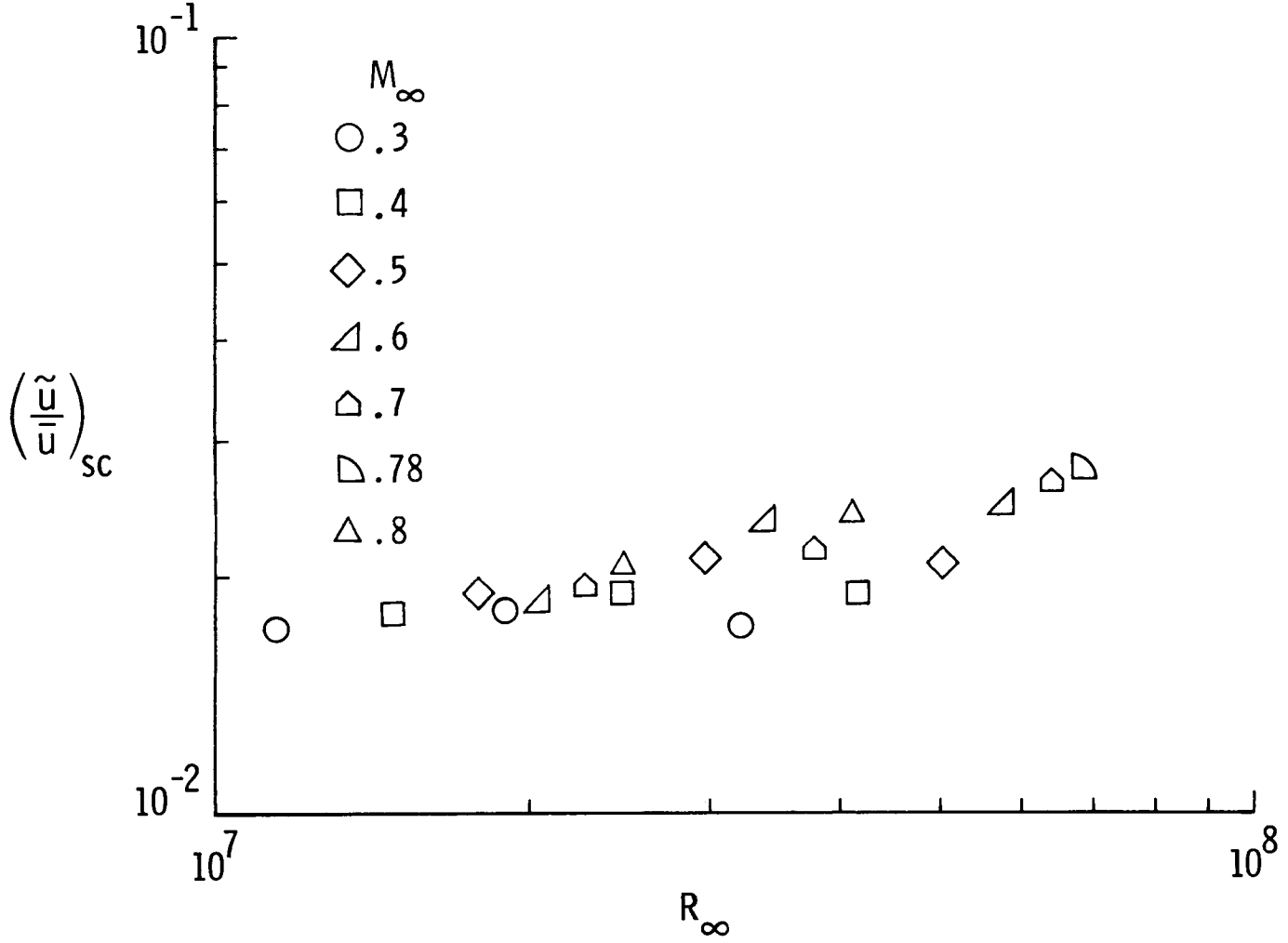

Figure 10.- Velocity fluctuation in settling chamber at cryogenic conditions. T_t = 140 K.

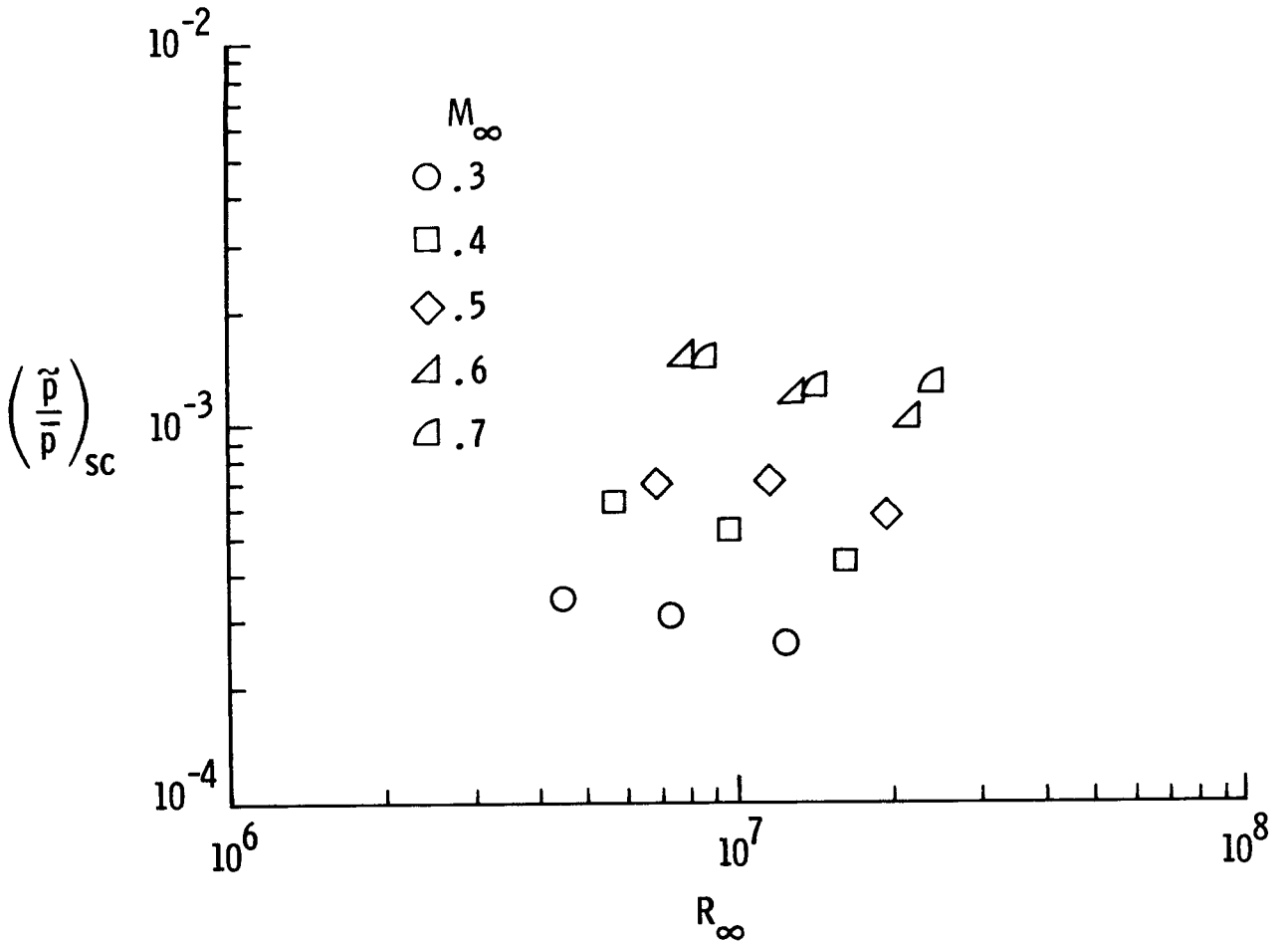

Figure 11.- Pressure fluctuations in settling chamber at near ambient conditions. T_t = 280 K.

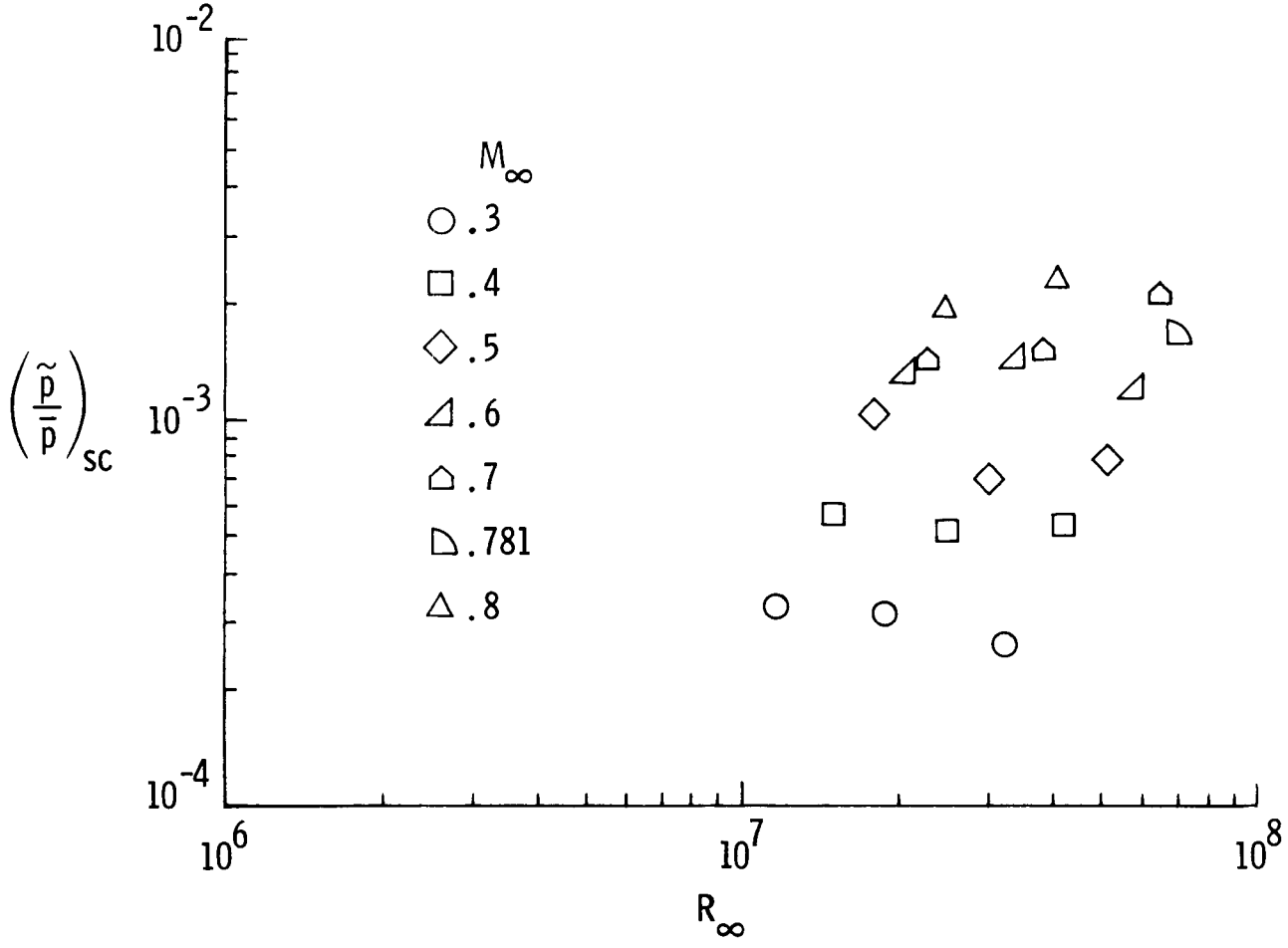

Figure 12.- Pressure fluctuations in settling chamber at cryogenic conditions. T_t = 140 K.

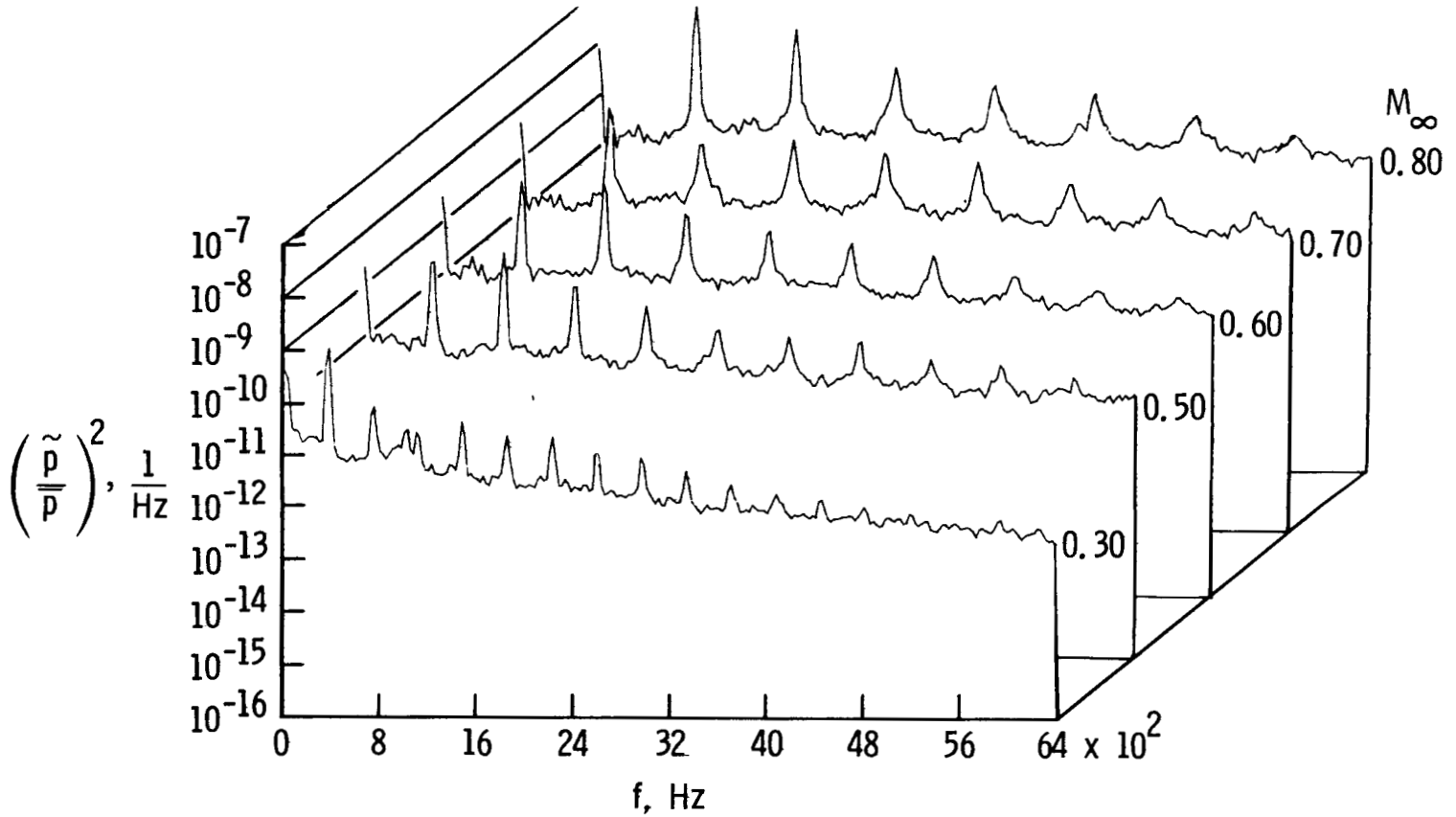

Figure 13.- Spectra of pressure fluctuations in settling chamber.
p_t = 3.4 atm; T_t = 140 K.

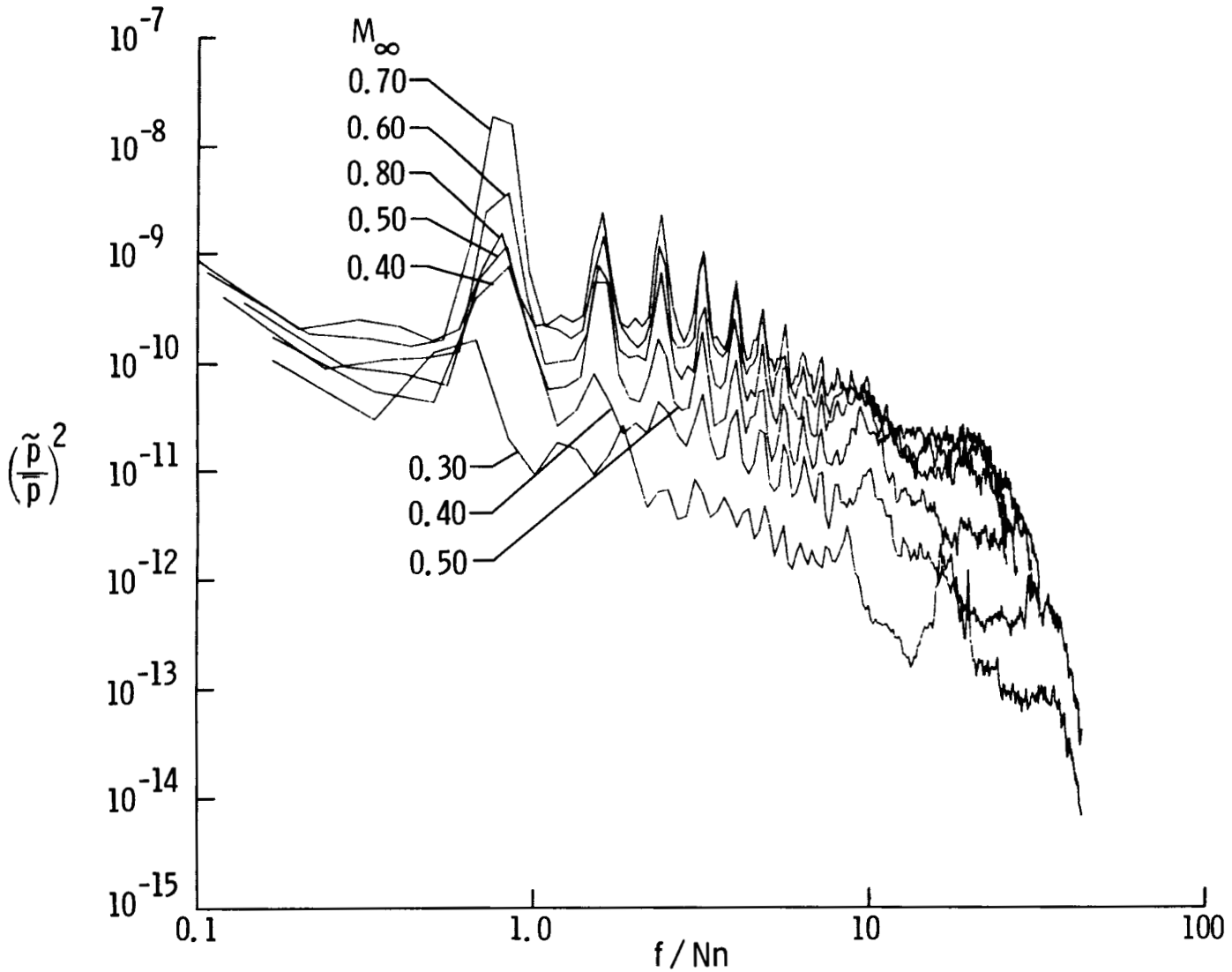

Figure 14.- Spectra of pressure fluctuations in settling chamber for dimensionless frequency. p_t = 5.8 atm; T_t = 140 K.

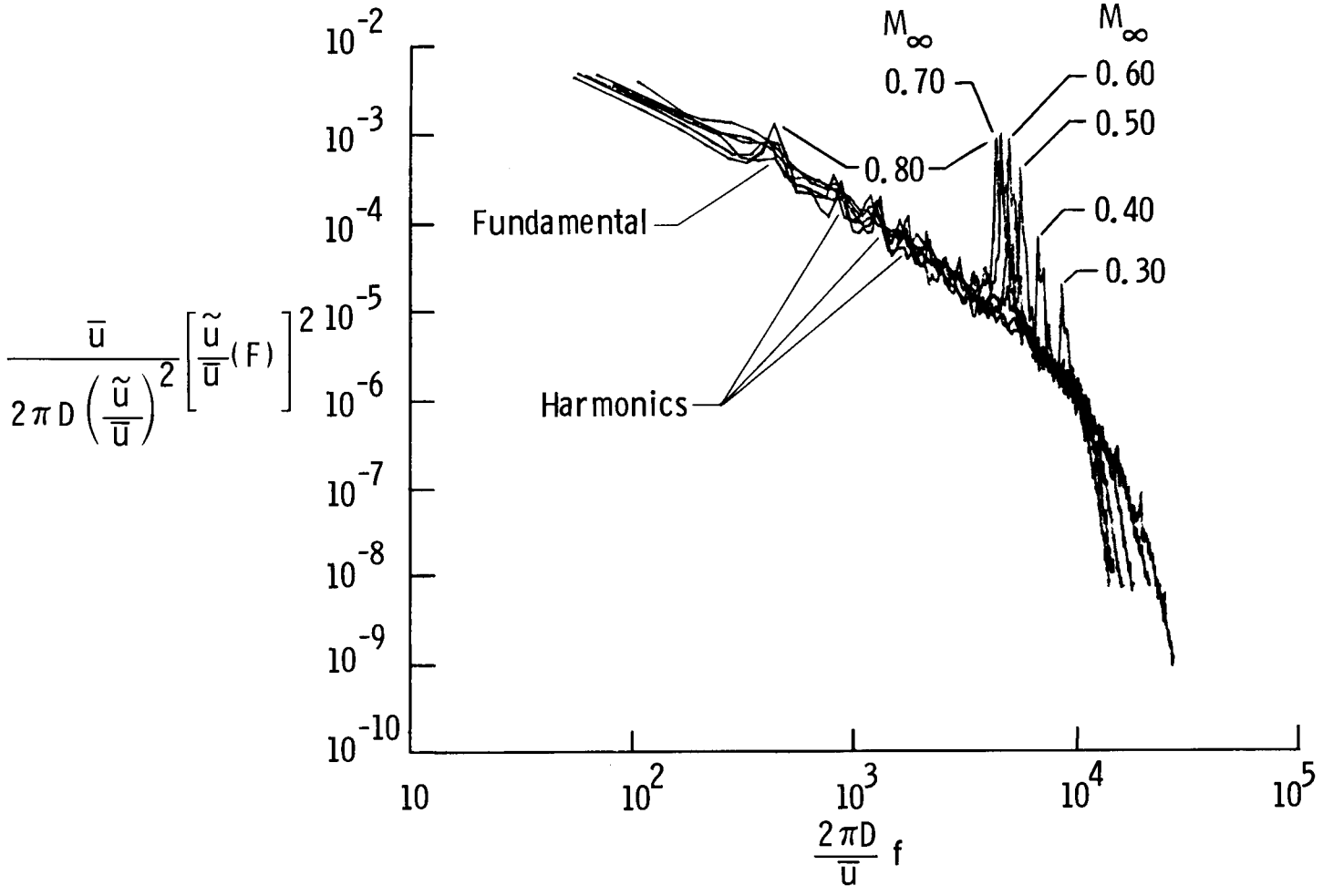

Figure 15.- Nondimensional spectra of velocity fluctuations in settling chamber at cryogenic conditions. p_t = 5.8 atm; T_t = 140 K.

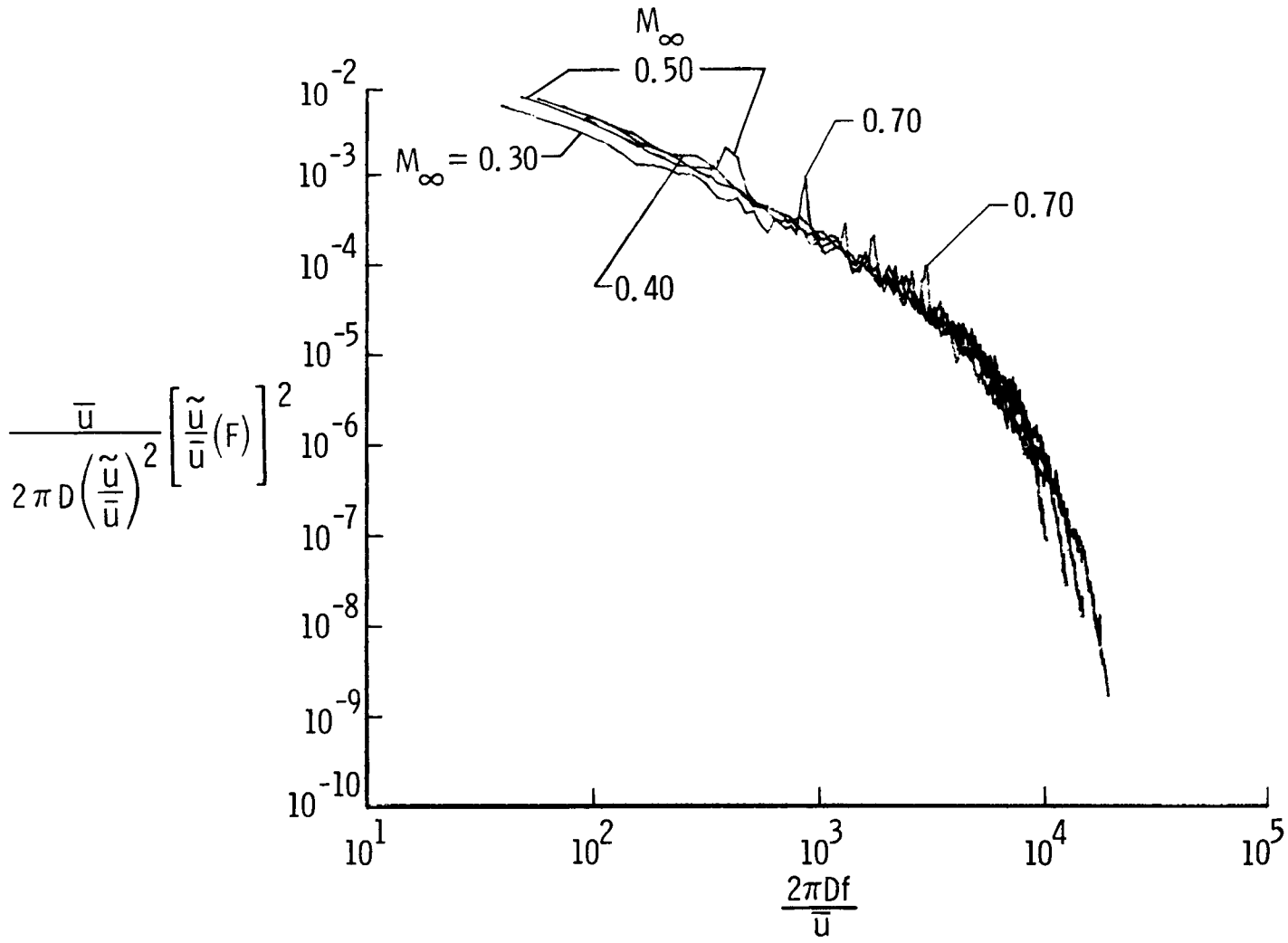

Figure 16.- Nondimensional spectra of velocity fluctuations in settling chamber at near ambient conditions. p_t = 5.8 atm; T_t = 280 K.

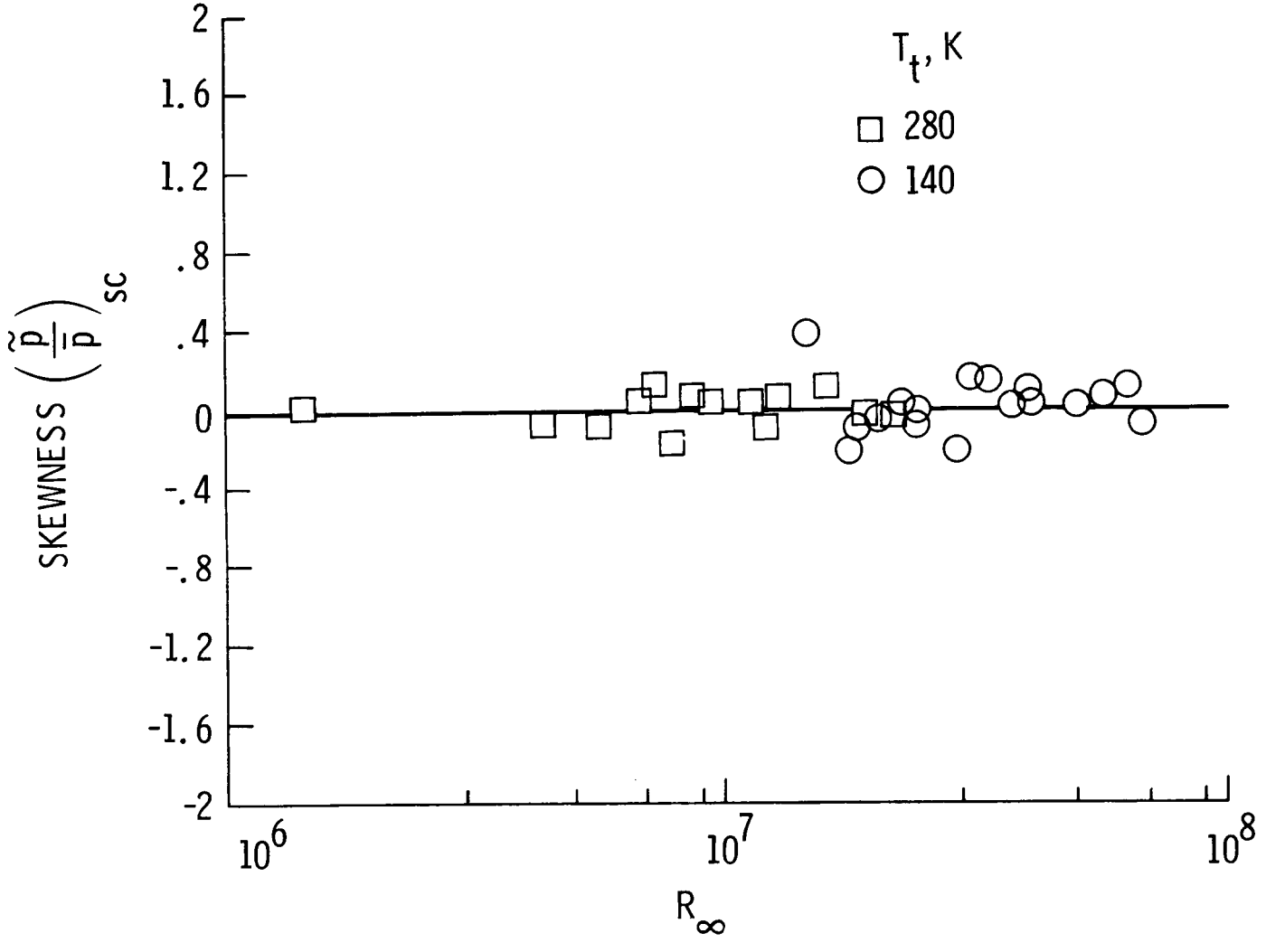

Figure 17.- Skewness of settling chamber pressure fluctuations.
$0.30 \leq M_\infty \leq 0.80$; $0.03 \leq M_{sc} \leq 0.06$.

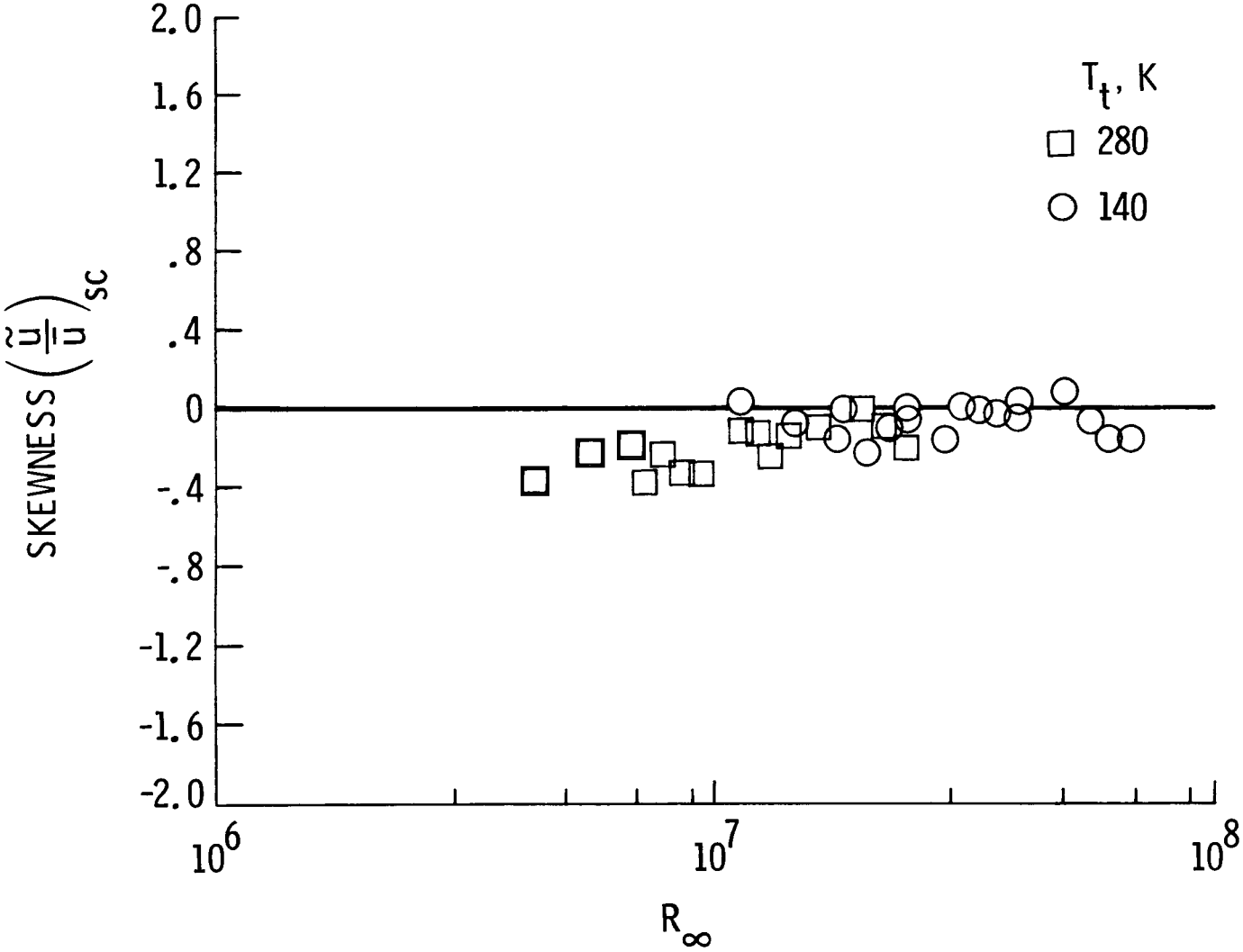

Figure 18.- Skewness of settling chamber velocity fluctuations.
$0.30 < M_\infty < 0.80$; $0.03 < M_{sc} < 0.06$.

Standard Bibliographic Page

1. Report No.	2. Government Accession No.	3. Recipient's Catalog No.
NASA TP-2584		

4. Title and Subtitle	5. Report Date
Dynamic Measurement of Total Temperature, Pressure, and Velocity in the Langley 0.3-Meter Transonic Cryogenic Tunnel	May 1986
	6. Performing Organization Code 505-61-01-02
7. Author(s)	8. Performing Organization Report No.
Charles B. Johnson and P. Calvin Stainback	L-16099
9. Performing Organization Name and Address	10. Work Unit No.
NASA Langley Research Center Hampton, VA 23665-5225	11. Contract or Grant No.
12. Sponsoring Agency Name and Address	13. Type of Report and Period Covered Technical Paper
National Aeronautics and Space Administration Washington, DC 20546-0001	14. Sponsoring Agency Code

15. Supplementary Notes

16. Abstract

An investigation was conducted in the Langley 0.3-Meter Transonic Cryogenic Tunnel to determine the possible existence of temperature fronts in the flow. Previous theoretical and experimental results indicated that a sudden or step increase or decrease in the rate of liquid nitrogen injection into the circuit of a cryogenic wind tunnel can cause a temperature front in the flow for several tunnel circuit times. Since these fronts can have an effect on the control of the tunnel as well as the time required to establish steady-flow conditions in the test section, measurements were made in the settling chamber with high response instrumentation to determine if there were temperature fronts. The results from three different techniques that suddenly changed the rate of liquid nitrogen injection indicate that temperature fronts do not appear to be present. Velocity and pressure fluctuations were also measured in the settling chamber.

17. Key Words (Suggested by Authors(s))	18. Distribution Statement
Cryogenic wind tunnels Velocity fluctuations Pressure fluctuations Total-temperature variation Hot wire	Unclassified - Unlimited Subject Category 09

19. Security Classif.(of this report)	20. Security Classif.(of this page)	21. No. of Pages	22. Price
Unclassified	Unclassified	43	A03

For sale by the National Technical Information Service, Springfield, Virginia 22161

NASA-Langley, 1986